Partial wave analysis of the $\pi^+\pi^-$ system produced in double gap p-p collisions at $\sqrt{s} = 7$ TeV

Taesoo Kim*, Ju Hwan Kang
Yonsei University

2016. 11. 26.

HIM Meeting, IBS

Overview

- Motivation of central diffraction
- Data analysis
- Partial wave analysis of $\pi^+\pi^-$ system
- Conclusion

Motivation: inelastic cross section

- Total cross section in p-p collisions
  - $\sigma_{\text{tot}} = \sigma_{\text{el}} + \sigma_{\text{INEL}}$, and σ_{INEL} increases faster than σ_{el} at high energies due to contributions from diffractive processes. Therefore, the diffraction can't be ignored at high energies.

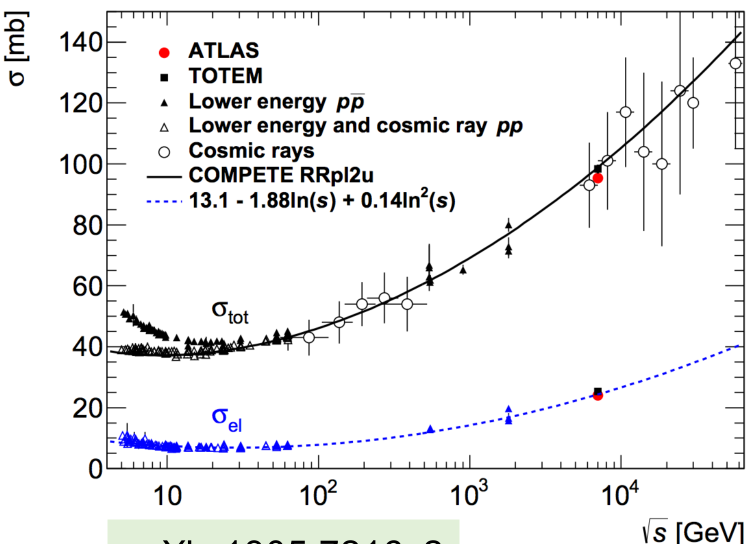

arXiv:1305.7216v2

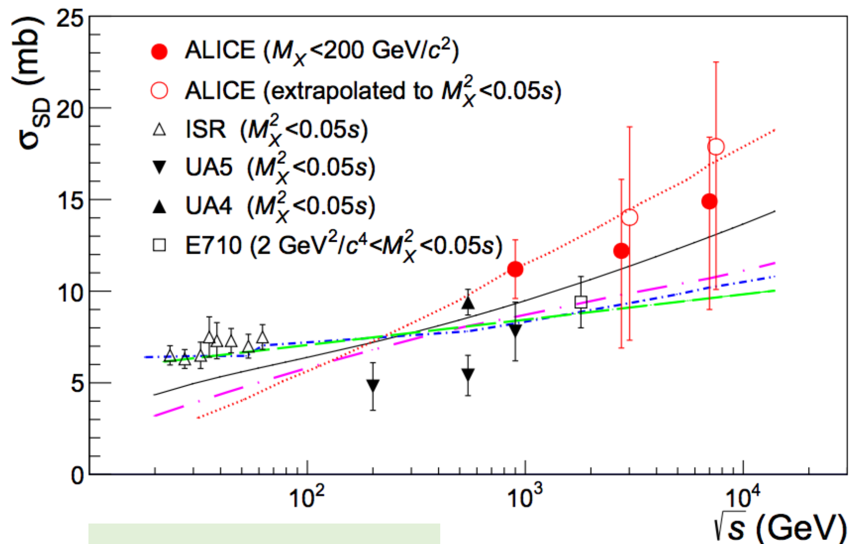

arXiv:1208.4968v1

  - $\sigma_{\text{INEL}} = \sigma_{\text{non-diff.(ND)}} + \sigma_{\text{single-diff.(SD)}} + \sigma_{\text{double-diff.(DD)}} + \sigma_{\text{central-diff.(CD)}} + \cdots$

$\sqrt{s}$ (TeV)	$\sigma_{SD}/\sigma_{INEL}$	$\sigma_{DD}/\sigma_{INEL}$
0.9	0.21 ± 0.03	0.11 ± 0.03
2.76	$0.20^{+0.07}_{-0.08}$	0.12 ± 0.05
7	$0.20^{+0.04}_{-0.07}$	$0.12^{+0.05}_{-0.04}$

SD+DD contribute 30% of INEL

arXiv:1208.4968v1 (ALICE)

Motivation: diffractive processes

- In Regge theory, all diffractive processes can be described by ***Pomeron*** at high energies.
  - ***Pomeron***: colour singlet object with the quantum number of the vacuum
  - While SD and DD are explained by single-Pomeron exchange,
    CD is dominated by double-Pomeron exchange (DPE).
- The diffraction is defined when the momentum transfer of incoming proton is much less than the centre-of-mass energy.
  - Single Diffraction (SD): one proton is intact and one proton dissociates, $p_1 + p_2 \rightarrow {p_1}' + X_2$
  - Double Diffraction (DD): two protons dissociate, $p_1 + p_2 \rightarrow X_1 + X_2$
  - Central Diffraction (CD): two protons are intact, $p_1 + p_2 \rightarrow {p_1}' + X + {p_2}'$

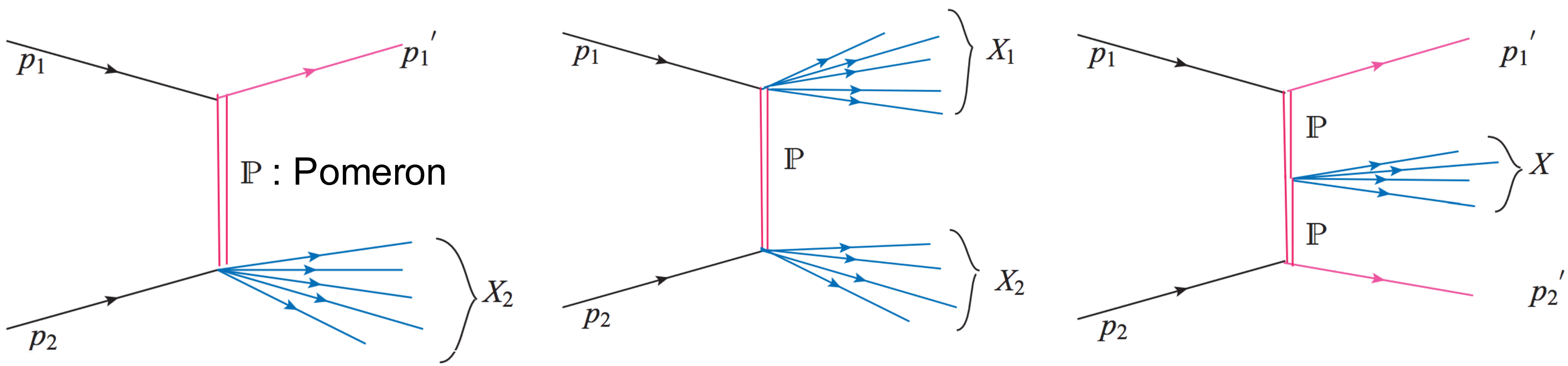

Feynmann diagrams of single (left), double (middle), and central (right) diffraction with Pomeron exchange, arXiv:1005.3894

Motivation: central diffraction (central production)

- Central diffraction, $p_1 + p_2 \rightarrow p_1{}' + X + p_2{}'$
  - ➢ produce interesting system X such as glueballs and hybrid due to glue-rich nature of Pomeron.
  - ➢ restrict the quantum numbers of the produced system X ($I^G J^{PC} = 0^{+}\mathrm{even}^{++}$), so final states can be $\pi^+\pi^-, K^+K^-, \pi^+\pi^-\pi^+\pi^-$, etc. The $\pi^+\pi^-$ had been analyzed in other experiments, $f_0(\mathbf{980})(J^{PC} = \mathbf{0}^{++})$ and $f_2(\mathbf{1270})(J^{PC} = \mathbf{2}^{++})$ are observed in the $\pi^+\pi^-$ final states.

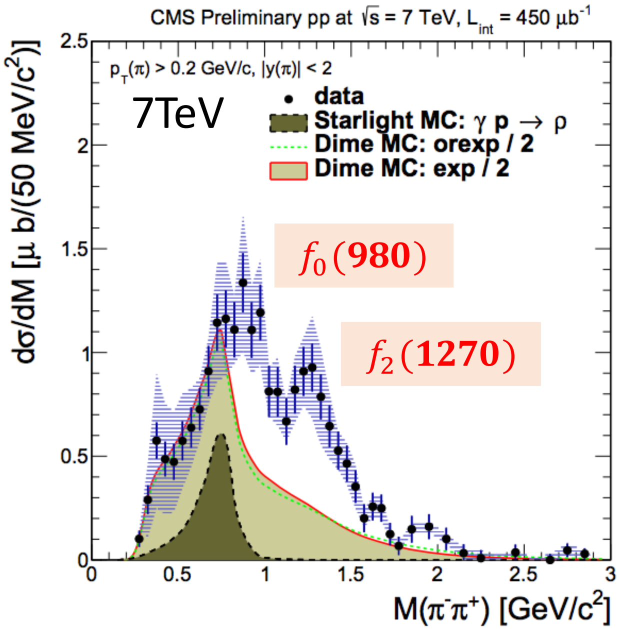

CMS result, arXiv:1610.08775v2

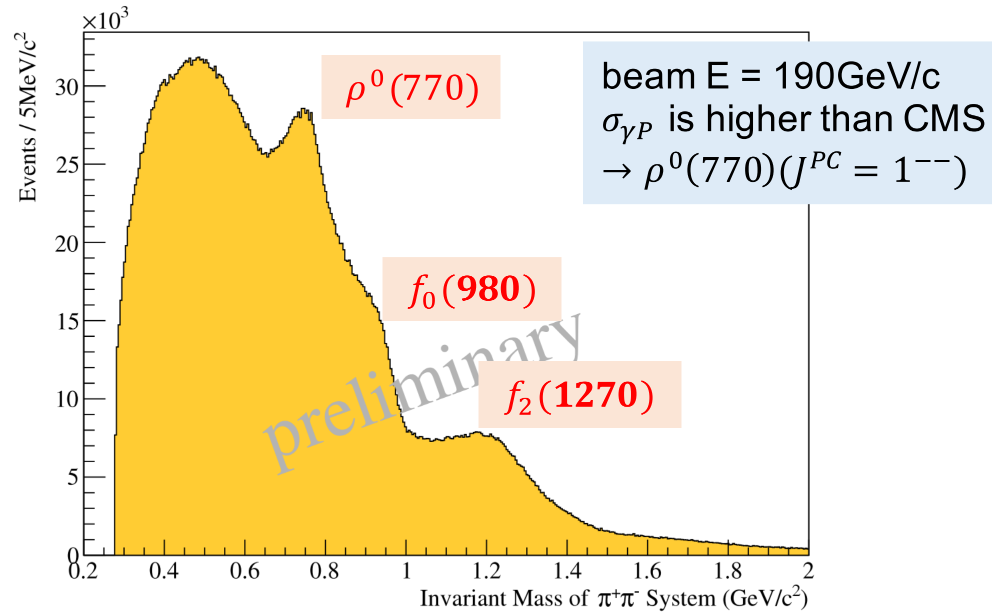

COMPASS result, arXiv:1310.3190v1

- The goal is to investigate $\pi^+\pi^-$ final states in CD and provide properties of produced particles.

Data analysis: double gap topology

- Even though A Large Ion Collider Experiment (ALICE) is dedicated experiment for heavy-ion collisions, ALICE is suitable for investigating central diffraction in p-p collisions.
- Double gap topology
  - $p_1 + p_2 \to p_1{}' + X + p_2{}'$ can be identified if all protons are measured.
  - ALICE can't detect outgoing protons ($p_1{}', p_2{}'$) due to absent of very forward detectors.
  - Alternatively, we can use **double gap (DG) topology** to identify CD.
    - While intact protons have large pseudorapidity (η), the produced system X has very small η because of small momentum transfers.
    - Thus, we have two gaps between intact protons and the produced system X.

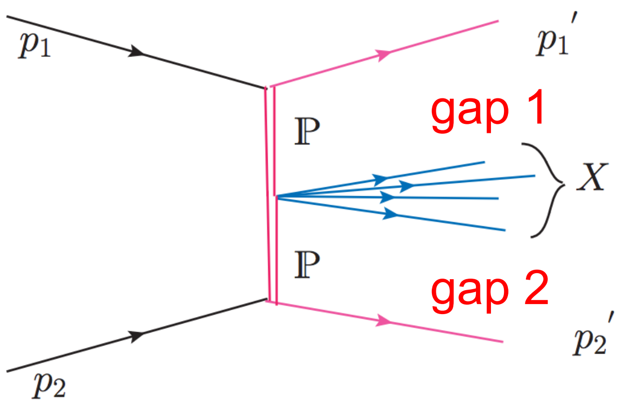

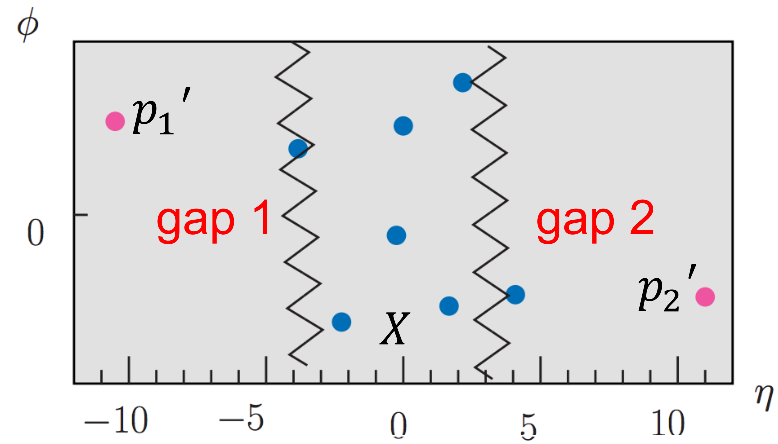

Central diffraction with DPE and rapidity distribution of produced particles, arXiv:1005.3894

Data analysis: ALICE detectors

- Double gap topology in ALICE as a trigger
  - This trigger was not implemented as online in Run1. Therefore, we use offline information to reconstruct the DG trigger.
  - <u>*Requirement:* ***some signals in central regions without any activities in forward gaps***.</u>
  - ALICE has V0, FMD at forward regions to detect gaps and SPD to measure centrally produced signal as trigger detectors.
  - DG in ALICE: !V0C & !V0A & SPD, where & (!) is logical AND (NOT)
    - No signals on V0A,C side and at least one fired chip in SPD
    - Sub-sample: !FMDC & !V0C & !FMDA & !V0A & SPD (enhanced gap definition)

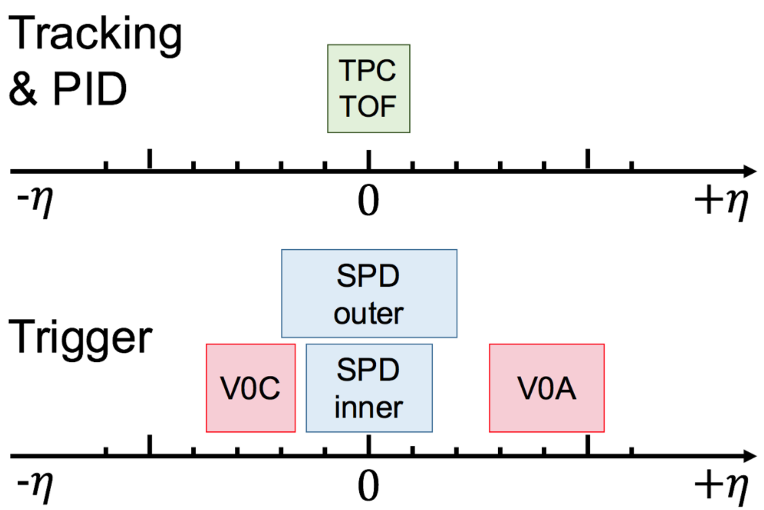

TPC: $-0.9 < \eta < 0.9$
SPD outer layer: $-2 < \eta < 2$
SPD inner layer: $-1.4 < \eta < 1.4$
V0A: $2.8 < \eta < 5.1$
V0C: $-3.7 < \eta < -1.7$
<u>FMDA: $1.7 < \eta < 5.1$</u>
<u>FMDC: $-3.4 < \eta < -1.7$</u>

Data analysis: ALICE detectors

- Trigger: V0, Forward Multiplicity Detector (FMD), Silicon Pixel Detector (SPD)
- Tracking: Inner Tracking System (ITS) + Time Projection Chamber (TPC)
- Particle Identification (PID) :ITS, TPC, Time Of Flight (TOF)

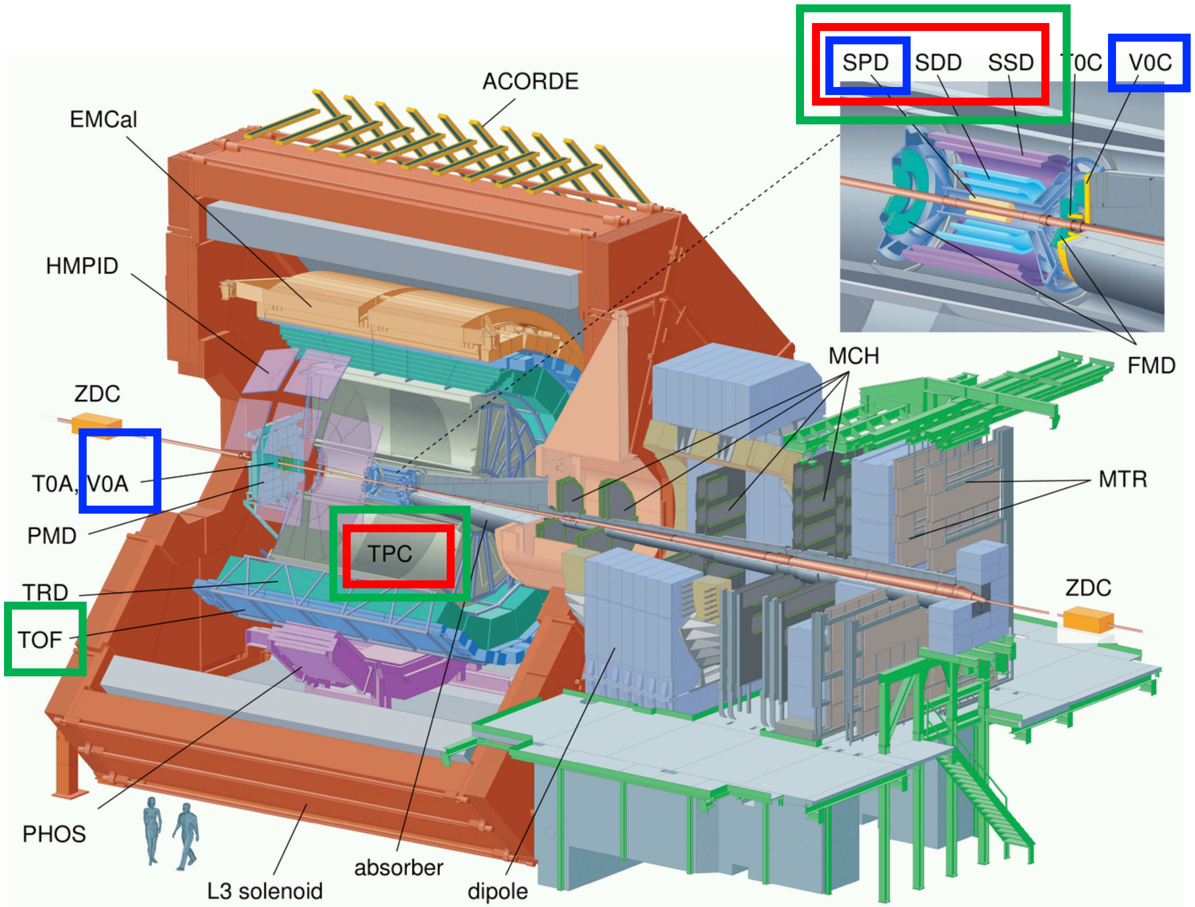

ALICE shcematic view, arXiv:1402.4476

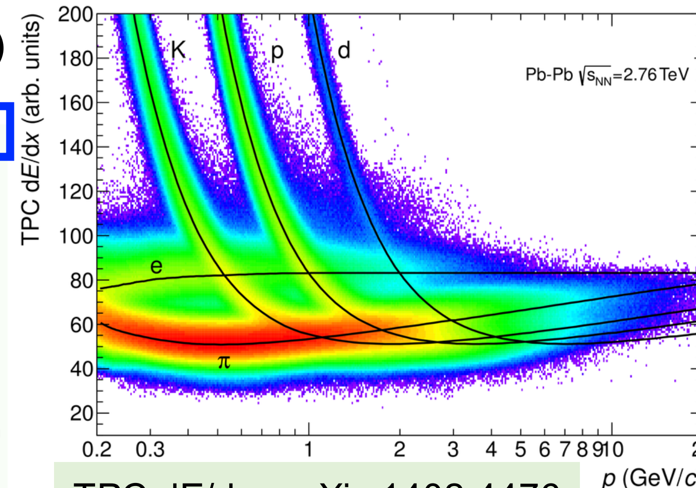

TPC dE/dx, arXiv:1402.4476

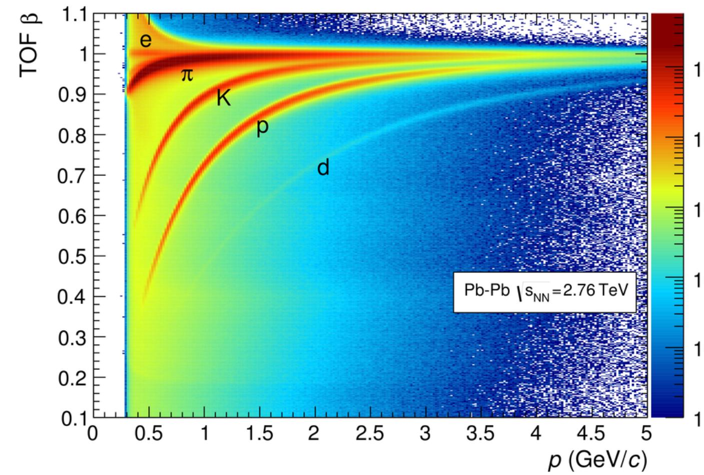

TOF particle velocity, arXiv:1402.4476

Data analysis: dataset

- Dataset
  - LHC10b, c, d, e, f pass4 (all available data in p-p collisions at $\sqrt{s} = 7$ TeV)
  - Minimum bias trigger in ALICE
    - $\mathrm{MB_{OR}}$: V0C || V0A || SPD, where || is logical OR (Total # ~ 418M)
    - Note that DG is defined only in $\mathrm{MB_{OR}}$
  - Double gap using V0+SPD: !V0C & !V0A & SPD (Total # ~ 1.5M)
- Run quality analysis to evaluate the ratio of the DG triggers, $R_{\mathrm{DG,V0}} = N_{\mathrm{DG,V0}}/N_{\mathrm{MB_{OR}}}$.

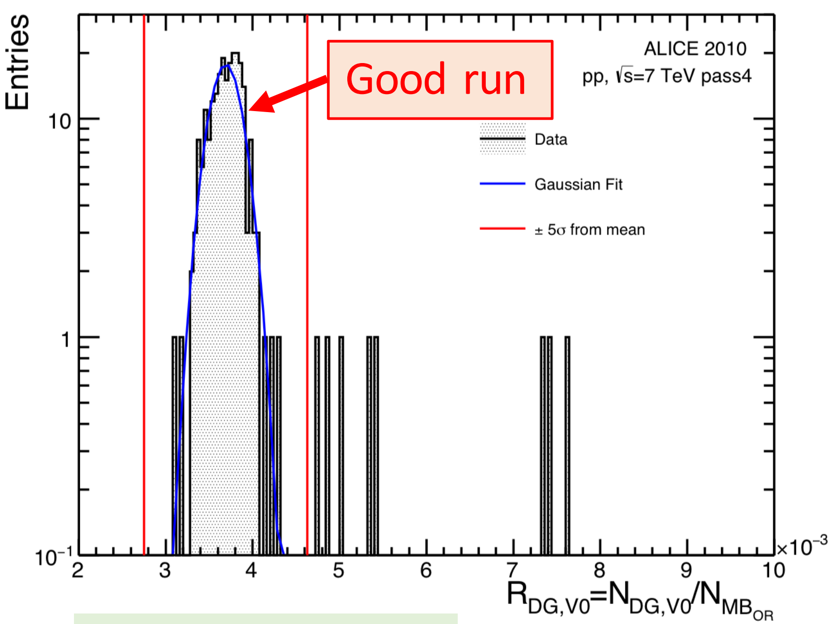

Distribution of $R_{\mathrm{DG,V0}}$

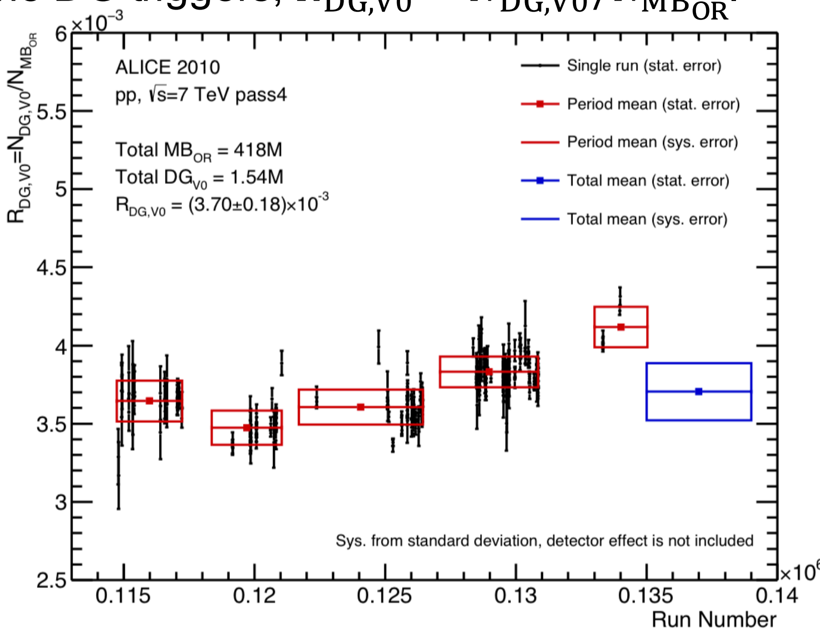

$R_{\mathrm{DG,V0}}$ as a function of run numbers and it is stable

Data analysis: event and track selection

- Event selection procedures to reject pile-up and beam-gas events.

Procedures	# of events (%)
MB_{OR} offline	418M (100%)
Vertex cut, $\|z_{vtx}\| < 10$ cm	345M (83%)
Pile-up rejection using secondary SPD vertex	336M (80%)
SPD $N_{clusters}$ vs. $N_{tracklets}$	336M (80%)
Double-gap	0.98M (0.2%)

- Trackcuts: Standard trackcuts + More trackcuts to select only N-track events

Standard trackcuts	Value
# of clusters in TPC (LHC10d,e,f)	> 70
# of crossed rows in TPC (LHC10b,c)	> 70
Ratio crossed rows over findable clusters in TPC (LHC10b,c)	> 0.8
Chi2 per cluster in TPC	< 4
Accept kink daughter	false
Require TPC, ITS refit	true
Cluster requirement in ITS	kSPD,kAny
DCA to vertex X,Y p_T dependency	$0.0182+0.0350/p_T^{1.01}$
Chi2 of TPC constrained global	< 36
DCA to vertex Z	< 2 cm
DCA to vertex 2D	false
Require sigma to vertex	false

More trackcuts	Value
# of shared cluster in TPC	< 3
Distance between z_{trk} and z_{vtx}	< 6 cm
Eta of track	-0.9 to 0.9
No unassociated tracklet for selected track	
No unassociated SPD fired chip for selected track	
PID: Bayesian probabilities are used P_p or P_K > 95% are rejected P_π < 60% are rejected	

Data analysis: event and track selection

- Global track in ALICE: $-0.9 < \eta < 0.9$
- Another definition of track in ALICE: tracklet
  - A line between one point in SPD inner layer and another point in SPD outer layer
  - Eta of tracklet : $-2 < \eta < 2$

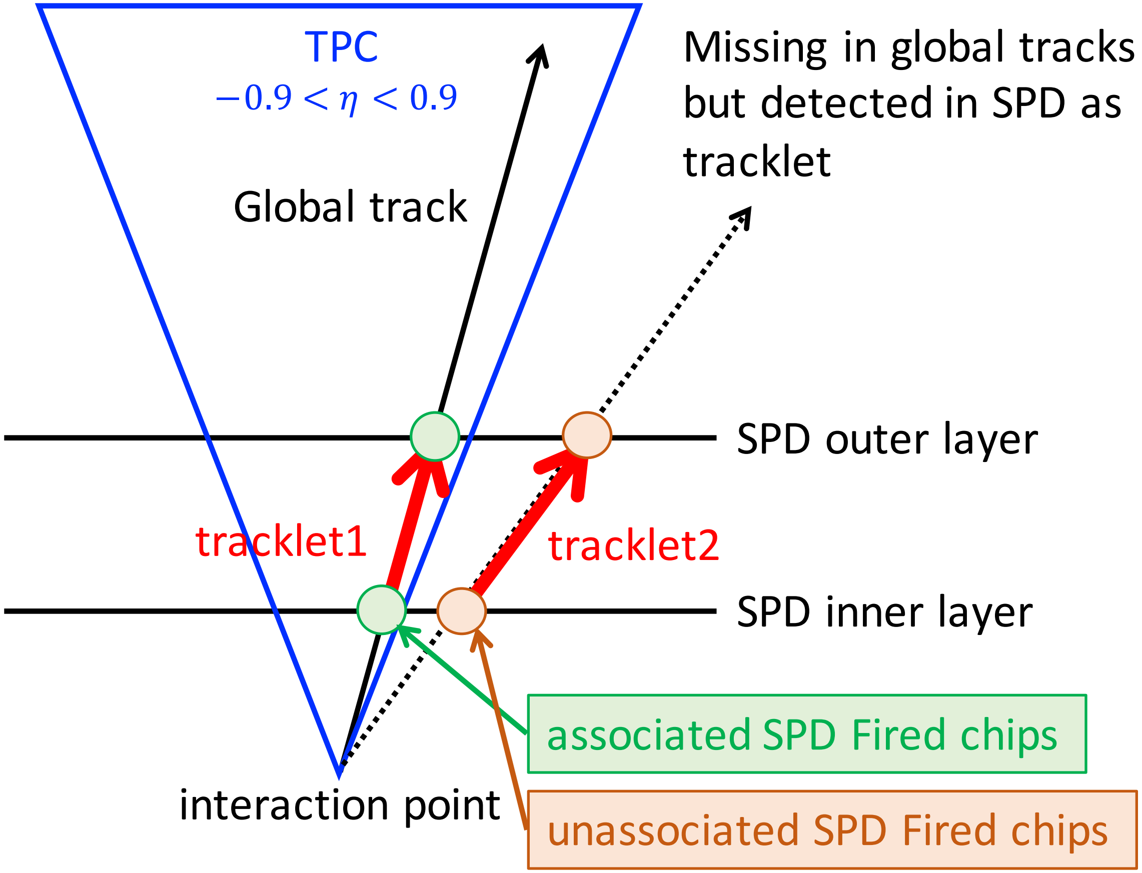

1. $N_{\text{tracklets}} > N_{\text{tracks}}$: rejected
This means we required no activities outside of TPC regions to enhance gap definitions.
Before, no signals in

$$2.8 < \eta < 5.1$$
$$-3.7 < \eta < -1.7$$

Now, we can have more gaps in

$$-2.0 < \eta < -0.9$$
$$+0.9 < \eta < +2.0$$

additionally.

2. unassociated SPD fired chips : rejected
reduce noisy SPD chips ensuring signals are from tracks

Data analysis: raw multiplicity distribution

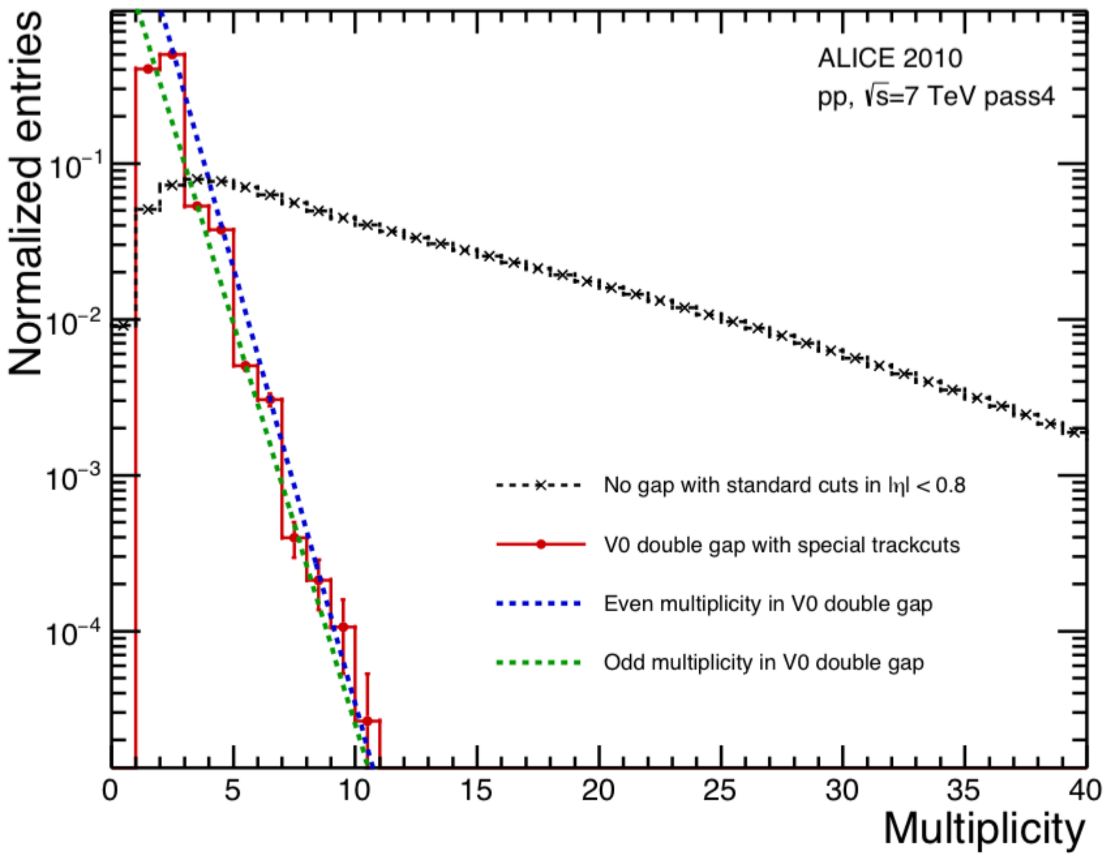

X-axis : Multiplicity
Y-axis : Normalized entries

Black = No gap
Red = V0 double gap
Blue = Even number in V0 DG
Green = Odd number in V0 DG

- No gap (NG) event can be used as comparison because this refers non-diffractive events.
  - NG: !DG & !Single gap A-side & !Single gap C-side
- DG shows clear difference with NG events and has very small multiplicities for all events.
- More of even-multiplicity events than odd-multiplicity events (DPE produce only even multiplicities) → DG triggers pick up DPE process as well as background.

Data analysis: raw invariant mass distribution of $\pi^+\pi^-$

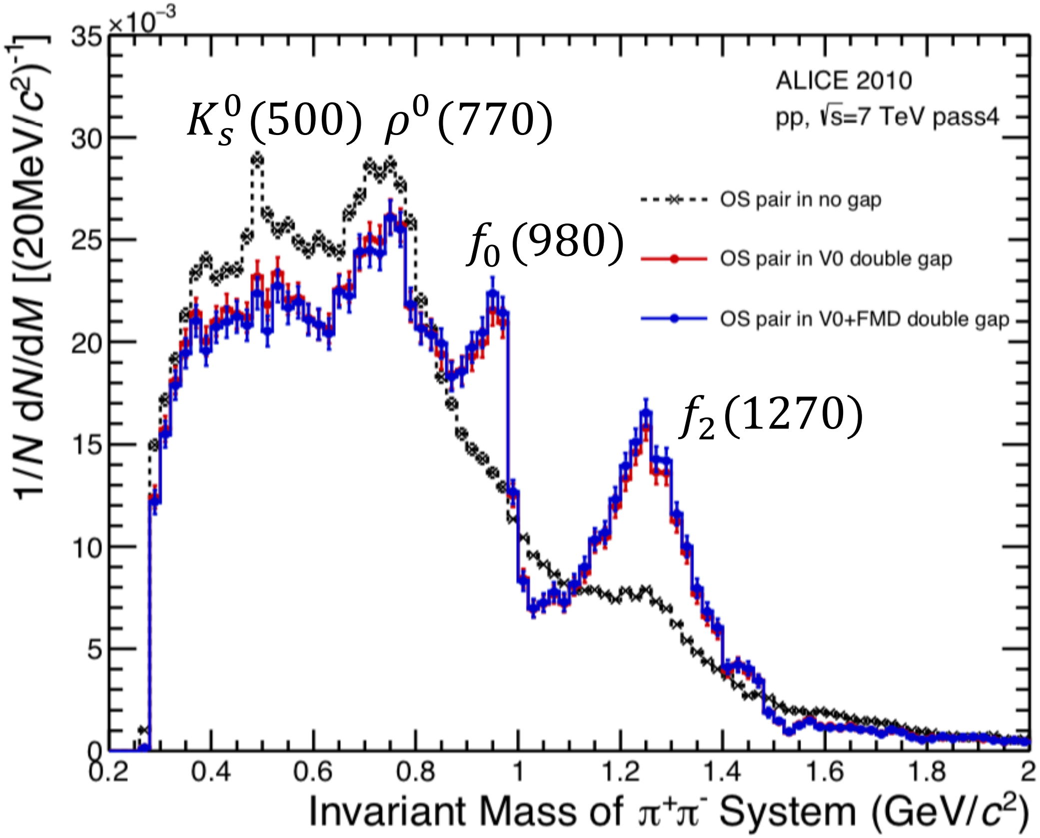

X-axis : Invariant mass of $\pi^+\pi^-$
Y-axis : Normalized entries

Black = No gap
Red = V0 double gap (~40K)
Blue = V0+FMD double gap (~35K)

$\rho^0(770)$ appeared in DG which is not allowed in DPE process
1. photon-Pomeron interaction
2. Feed-down from 3- or 4- body decay
3. Pure background

- Like-sign contamination is very low ~ 3% of total two-pion events.
- Again, NG is used as comparison and it has $K_s^0(500)$ and $\rho^0(770)(J^{PC} = 1^{--})$.
- There are clear signals of $f_0(980)$ and $f_2(1270)$ in both V0 and V0+FMD gaps and no difference between these two gaps. → V0 gap can be used for further analysis due to large statistics.
- DG contains DPE process with $\pi^+\pi^-$ final states as well as background.

Data analysis: p_T distribution of $\pi^+\pi^-$

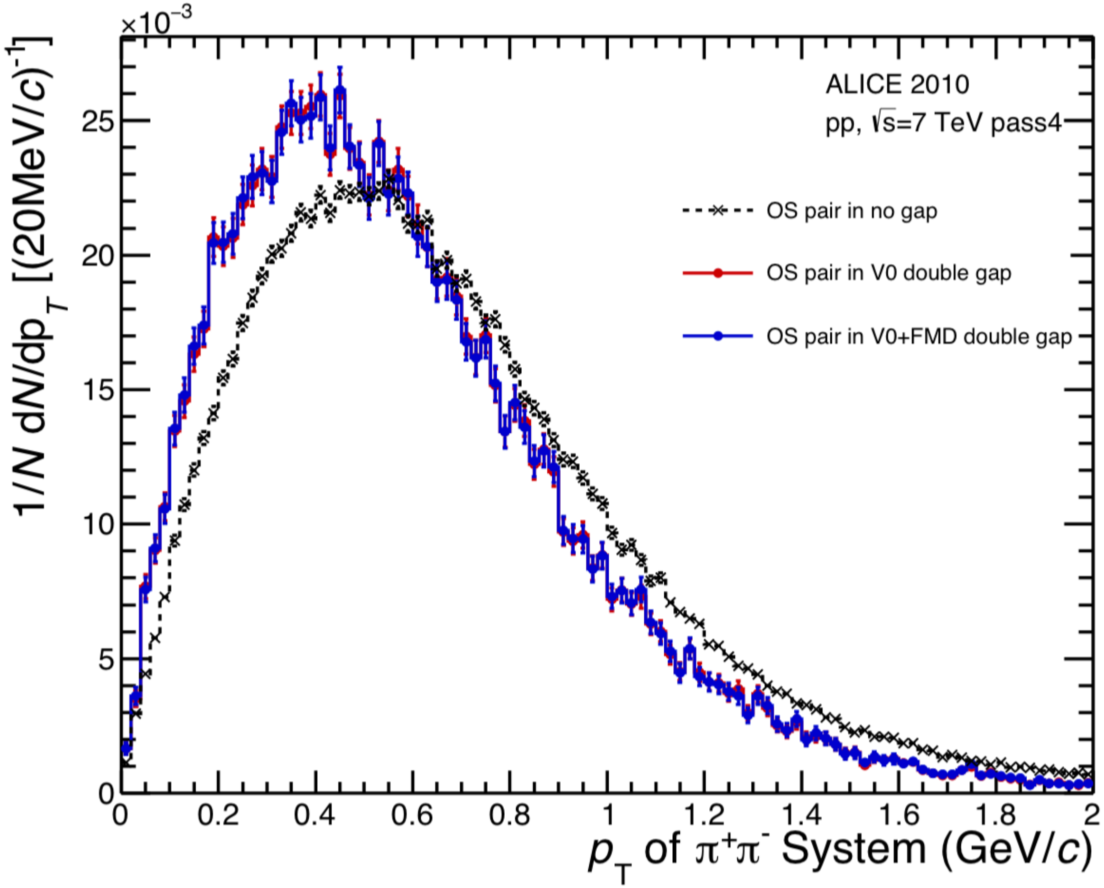

X-axis : p_T of $\pi^+\pi^-$
Y-axis : Normalized entries

Black = No gap
Red = V0 double gap (~40K)
Blue = V0+FMD double gap (~35K)

- As DPE is related to small momentum transfer in transverse plane, p_T of produced system should be very small.
- Mean p_T of DG is smaller than NG and there is no difference between V0 and V0+FMD gaps.
  - DG contains DPE process with $\pi^+\pi^-$ final states as well as background.

Data analysis: estimation of background

- Even though DG selects the DPE process, there is a chance that other processes are triggered with DG as background.
  - $\boldsymbol{N_{\mathrm{DG},2\pi}} = \boldsymbol{N_{\mathrm{CD},2\pi}} * \boldsymbol{\epsilon_{\mathrm{CD},2\pi}} + \boldsymbol{N_{\mathrm{NCD},2\pi}} * \boldsymbol{\epsilon_{\mathrm{NCD},2\pi}}$, where NCD means non central diffraction.
    - NCD = ND+SD+DD+…
- To estimate amounts and shape of background, we used Pythia6 because Pythia6 doesn't have CD process at all.
  - Same track and event selections as data are applied to Pythia6.

- The goal is to get a purity of data samples and distinguish signal and background in the data.
- Purity of data sample
  - $P = \frac{N_{CD,2\pi} * \epsilon_{CD,2\pi}}{N_{DG,2\pi}} = \frac{N_{DG,2\pi} - N_{NCD,2\pi} * \epsilon_{NCD,2\pi}}{N_{DG,2\pi}} = \frac{Data - Pythia6}{Data}$
  - Analysis of backgrounds from other sources is ongoing using Pythia8, PHOJET and STARLIGHT
    1. Feed down from high mass central diffraction (Pythia8, PHOJET)
    2. $\rho^0(770)$ from photon-Pomeron interaction (STARLIGHT)

Data analysis: estimation of background

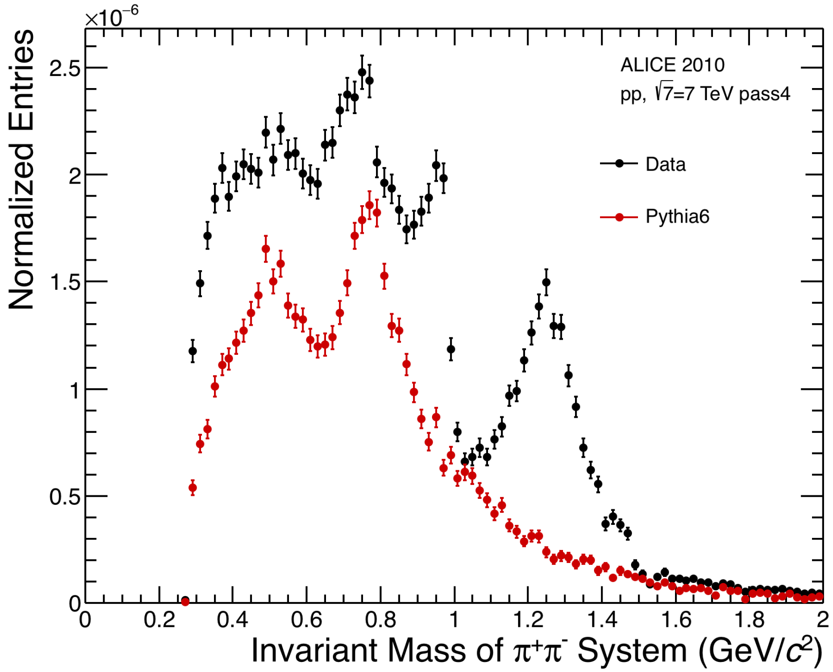

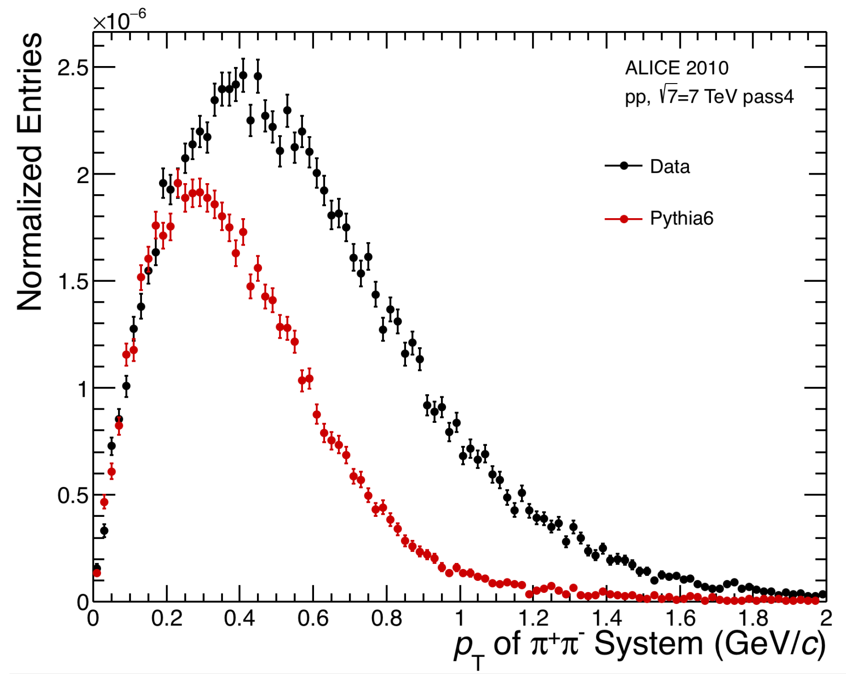

Invariant mass and p_T of $\pi^+\pi^-$ with data (black) and MC (Red). All histograms are normalized with each $N_{\mathrm{MB_{OR}}}$

- According to Pythia6, there are large continuum non-resonant background below 1 GeV, and $\rho^0(770)$ from NCD is observed with the DG trigger.
  → Most of $\rho^0(770)$ in the data can be from NCD, not photon-Pomeron interaction.
  → This can explain why we observe $\rho^0(770)(J^{PC} = 1^{--})$ in DPE.
- We may use the cut on p_T in the data to distinguish signal and background, however, it is impossible to have a such cut.
  → It's hard to decompose signal and background in the data

Data analysis: estimation of background

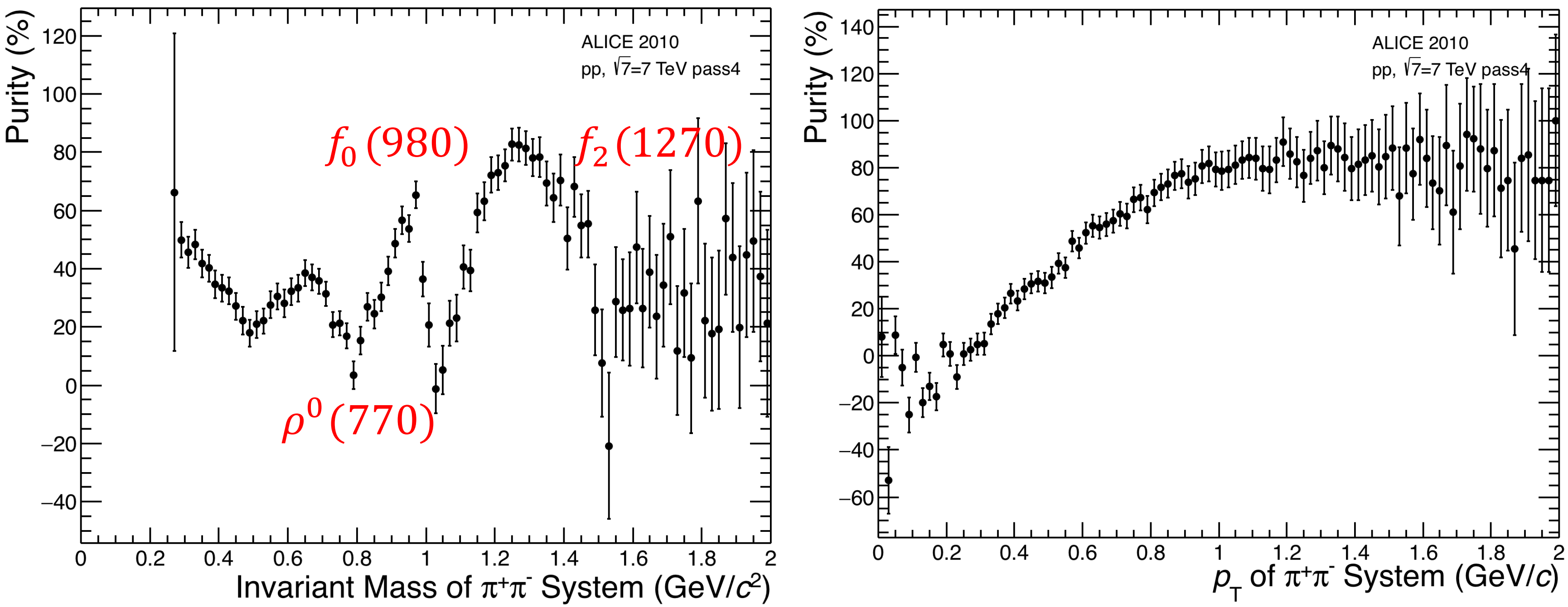

Purity as a function of an invariant mass (left) and p_{T} (right) of $\pi^+\pi^-$ system

- Purity of the data sample is about 60~80% at $f_0(980)$ and $f_2(1270)$, and almost 0% at $\rho^0(770)$.
  - Mean value of purity is around 50%.
  - If it is possible to get purities including backgrounds from other sources, cross section of $\pi^+\pi^-$ system can be obtained and compared with CMS.
- The higher the p_{T} is, the larger the purity is.
  - There is large amount of contamination of data sample in low p_{T} regions.
  - Note that this is model dependent.

Partial wave analysis: basic formalism

- In principle, invariant mass spectrum of $\pi^+\pi^-$ system is mixed with many meson states.
  - **Partial wave analysis (PWA)** allows to decompose particles into different quantum number states.
- Basic formalism †
  - PWA is tool to find out **'number of events of a given mass bin' having specific quantum number**
    - Partial amplitudes: $\boldsymbol{J^{\epsilon}_{M}}$, where J is spin, ϵ is reflectivity, and M is magnetic quantum number
      e.g. $S_0^-, D_0^-, D_1^-, D_1^+, \dots$ (complex number)
    - **Number of particles in one mass bin = $|\boldsymbol{J^{\epsilon}_{M}}|^2$**
  - Likelihood function for finding '***n***' events of a given bin with a finite acceptance $\eta(\Omega)$:
    - $L = \left[\frac{\bar{n}^n}{n!} e^{-\bar{n}}\right] \prod_i^n \left[\frac{I(\Omega_i)}{\int I(\Omega)\eta(\Omega)d\Omega}\right]$
  - By applying extended log-likelihood method, equation is simplified to minimizing function F.
    - $F = -\sum_i \ln \boldsymbol{I(\Omega_i)} + \sum_{LM} \boldsymbol{t_{LM}} \boldsymbol{\epsilon_{LM}}$, where i is event number and (L,M) are quantum numbers.
    - **Angular distribution from the data:** $\boldsymbol{I(\Omega_i)} = \sum_{LM} \boldsymbol{t_{LM}} \mathrm{Re} Y_L^M(\Omega_i)$
      ,where Y_L^M is a spherical harmonic function and Ω_i is solid angle of π^+ in GJ frame.
    - **Efficiency term from MC:** $\epsilon_{LM} = \frac{4\pi}{N_{gen}} \sum_j \mathrm{Re} Y_L^M(\Omega_j)$, for acceptance correction
    - $\boldsymbol{t_{LM}}$**: fit parameters**, but can be exchanged to partial wave components, J^{ϵ}_{M}.
    - Minimizing F using `Minuit(MIGRAD)` in `ROOT`

† Suh-Urk Chung, "Techniques of Amplitude Analysis for Two-pseudoscalar Systems", Physical Review D56, 7299, 1997

Partial wave analysis: correlation between fit parameters

- t_{LM} have correlations with partial amplitudes and we can obtain J_M^{ϵ} doing PWA.

$$
\begin{aligned}
\sqrt{4\pi}t_{00} &= |S_0^-|^2+|P_0^-|^2+|P_1^-|^2+|P_1^+|^2+|D_0^-|^2+|D_1^-|^2+|D_1^+|^2+|D_2^-|^2+|D_2^+|^2 \\
\sqrt{4\pi}t_{10} &= \frac{2}{5}(\sqrt{15}D_1^+P_1^+ + \sqrt{15}D_1^-P_1^- + 5P_0^-S_0^- + 2\sqrt{5}P_0^-D_0^-) \\
\sqrt{4\pi}t_{11} &= \frac{\sqrt{2}}{5}(\sqrt{15}D_2^+P_1^+ + \sqrt{15}D_2^-P_1^- + \sqrt{15}D_1^-P_0^- + 5P_1^-S_0^-) \\
\sqrt{4\pi}t_{20} &= \frac{1}{35}(\sqrt{5}(10|D_0^-|^2+5|D_1^-|^2+5|D_1^+|^2-10|D_2^-|^2-10|D_2^+|^2+14|P_0^-|^2-7|P_1^+|^2-7|P_1^-|^2) \\
&\quad +70D_0^-S_0^-) \\
\sqrt{4\pi}t_{21} &= \frac{\sqrt{2}}{35}(5\sqrt{15}D_2^+D_1^+ + 35S_0^-D_1^- + 5D_1^-(\sqrt{15}D_2^- + 7D_0^-) + 7\sqrt{15}P_0^-P_1^-) \\
\sqrt{4\pi}t_{22} &= \frac{1}{35\sqrt{2}}(70D_2^-S_0^- + \sqrt{15}(5|D_1^-|^2-5|D_1^+|^2+7|P_1^-|^2-7|P_1^+|^2) - 20D_0^-D_2^-) \\
\sqrt{4\pi}t_{30} &= \frac{6}{\sqrt{35}}(\sqrt{3}D_0^-P_0^- - D_1^+P_0^+ - D_1^-P_1^-) \\
\sqrt{4\pi}t_{31} &= \sqrt{\frac{3}{35}}(4D_1^-P_0^- + 6\sqrt{3}D_0^-P_1^- - D_2^+P_1^+ - D_2^-P_1^-) \\
\sqrt{4\pi}t_{32} &= \sqrt{\frac{6}{7}}(D_1^-P_1^- - D_1^+P_1^+ + P_0^-D_2^-) \\
\sqrt{4\pi}t_{33} &= \frac{3}{\sqrt{7}}(D_2^-P_1^- - D_2^+P_1^+) \\
\sqrt{4\pi}t_{40} &= \frac{1}{7}(6|D_0^-|^2-4|D_1^-|^2-4|D_1^+|^2+|D_2^-|^2+|D_2^+|^2) \\
\sqrt{4\pi}t_{41} &= -\frac{\sqrt{5}}{7}(D_1^+D_2^+ + D_1^-D_2^- - 2\sqrt{3}D_0^-D_1^-) \\
\sqrt{4\pi}t_{42} &= \frac{\sqrt{10}}{7}(|D_1^-|^2-|D_1^+|^2+\sqrt{3}D_0^-D_2^-) \\
\sqrt{4\pi}t_{43} &= \sqrt{\frac{5}{7}}(D_1^-D_2^- - D_1^+D_2^+) \\
\sqrt{4\pi}t_{44} &= \sqrt{\frac{5}{14}}(|D_2^-|^2-|D_2^+|^2)
\end{aligned}
$$

These terms have deep correlation with $M=2$ waves.
Our analysis results show these are compatible to zero, therefore, we can ignore $M=2$ waves.

Partial wave analysis: GJ'-frame

- Gottfried-Jackson frame is used as the coordinate system of PWA.
  - Pomeron mechanism
    - z-axis: $\overrightarrow{p_z}$ of incoming Pomeron in the $\pi^+\pi^-$ rest frame
    - y-axis: $\overrightarrow{p_z}\times\overrightarrow{p_X}$ in LAB frame
    - x-axis: $\overrightarrow{p_y}\times\overrightarrow{p_z}$ in the $\pi^+\pi^-$ rest frame
  - As we can't detect outgoing protons, we don't know momentum of Pomerons.
    → Proton mechanism, ignoring Pomeron in this case (GJ'-frame)
    - z-axis: $\overrightarrow{p_z}$ of incoming proton in the $\pi^+\pi^-$ rest frame

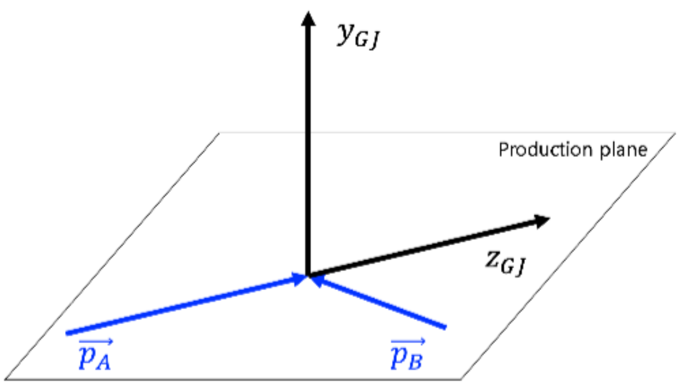

GJ'-frame with production plane

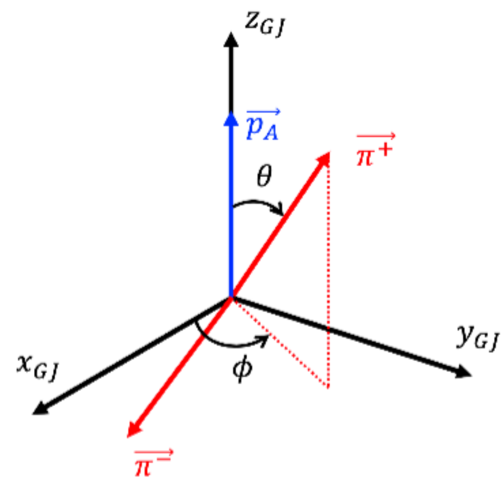

GJ'-frame with definition of solid angle

Partial wave analysis: $I(\Omega_i)$ in minimizing function F

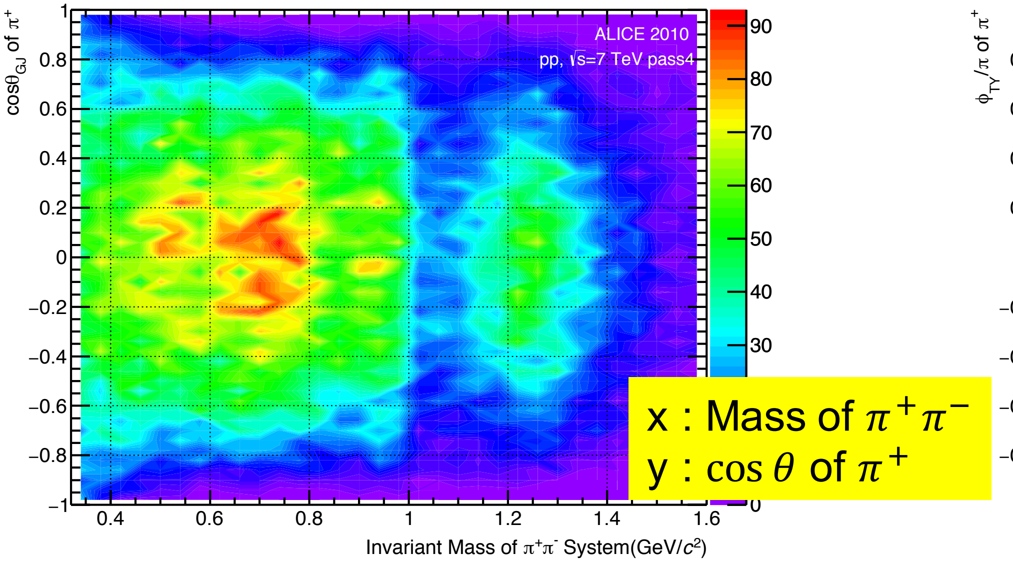

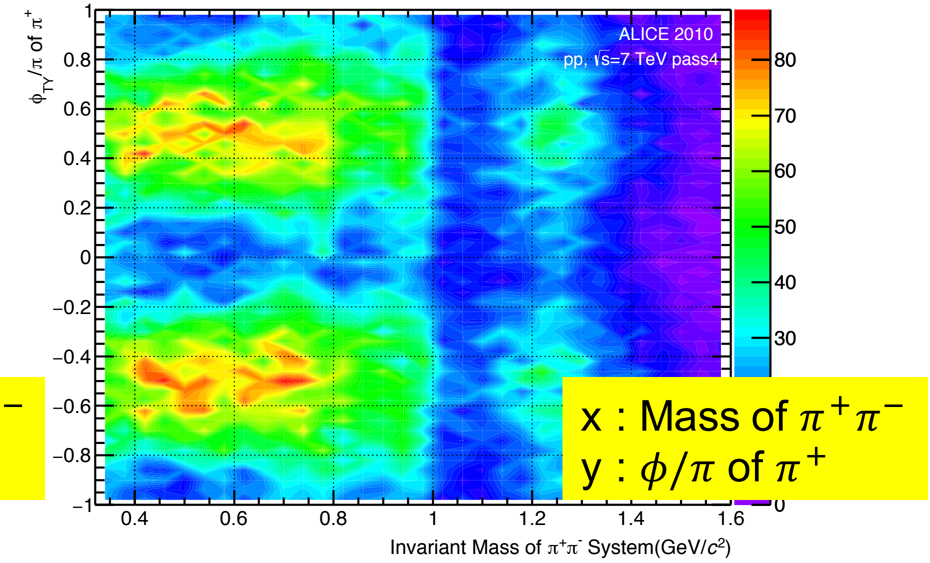

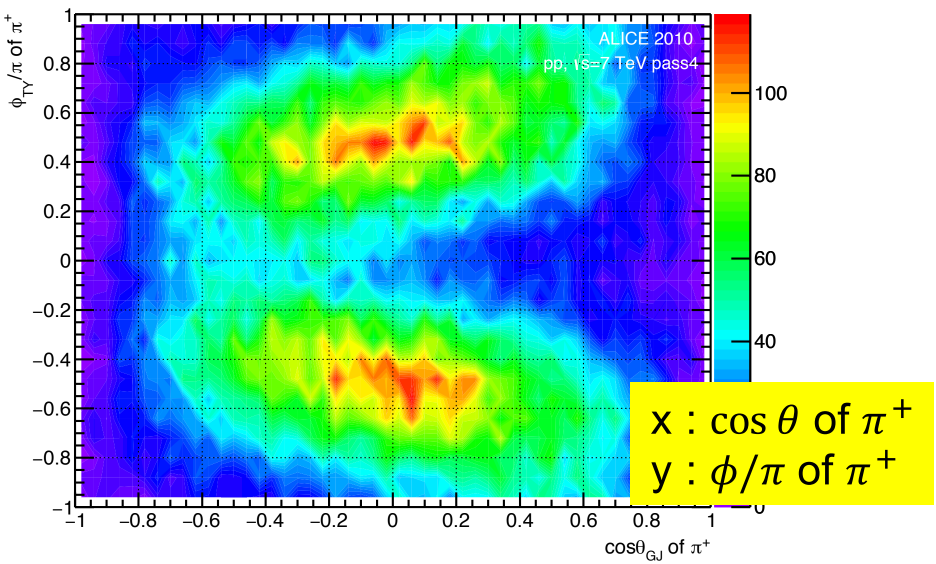

Raw angular distributions in the data. These are decomposed to different partial amplitudes according to spherical harmonics with acceptance correction using PWA.

Partial wave analysis: ϵ_{LM} in minimizing function F

- **MC set**: special generator is prepared for partial wave analysis
  - Generator: DRgen from COMPASS, $p + p \to p + X + p \to p + \pi^+\pi^- + p$
    - system X is produced from double-Pomeron exchange and decay to only $\pi^+\pi^-$
  - Generated system has $|y_{X,Gen.}| < 2$, however, $|y_{X,Gen.}| < 1$ is applied to impose proper condition of CEP
- ϵ_{LM} roughly means acceptance X efficiency for (L,M) quantum numbers

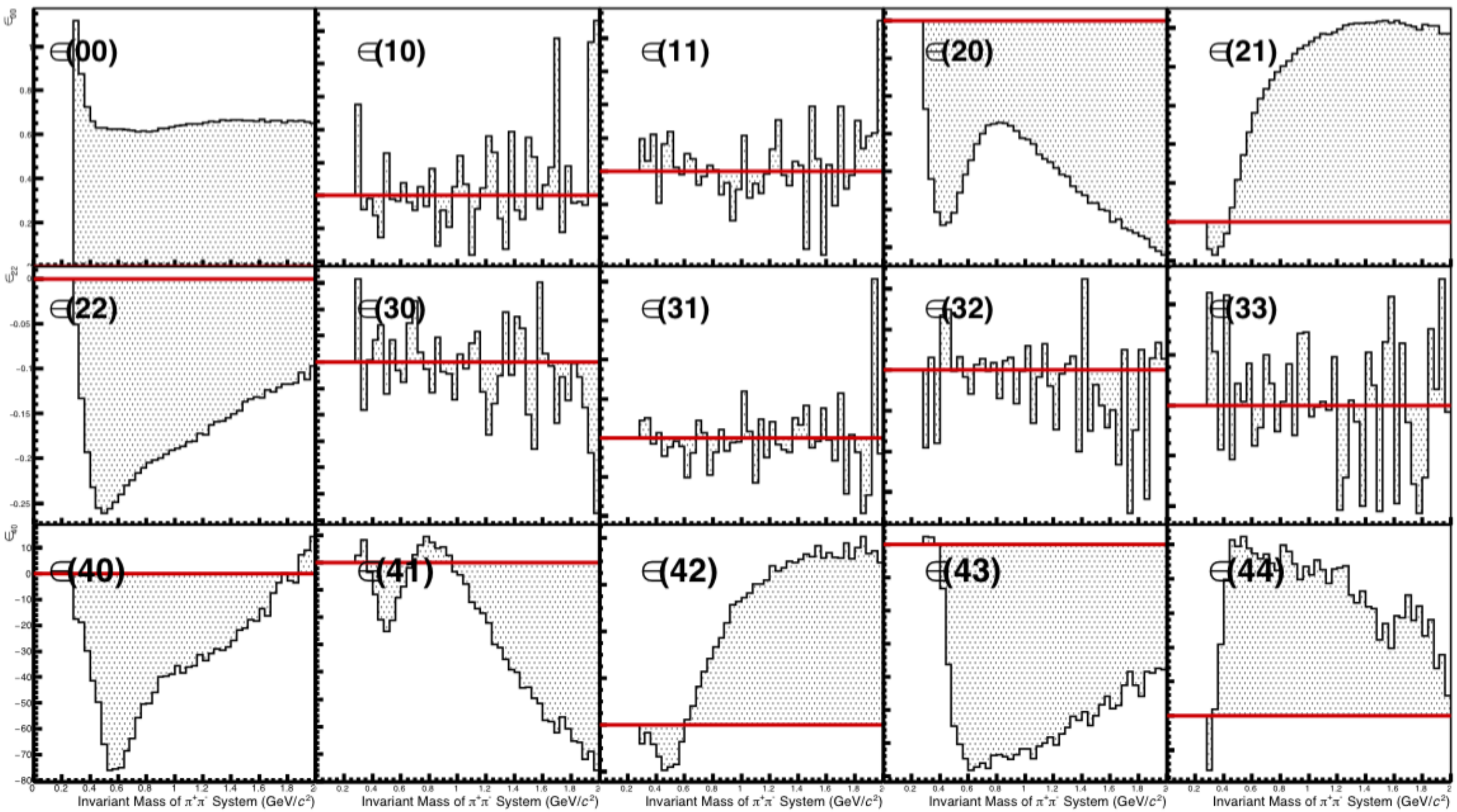

Partial wave analysis: Results

- Used wave-set = $S_0^-, D_0^-, D_1^-, D_1^+$ (spin 0,2)
  - $M = 2$ wave assumed to be zero based on t_{LM} results.
  - P-waves are not included to reduce uncertainties (DPE produce only even spin waves).
  - The reflectivity $-$ and $+$ don't interfere each other.
  - Width of mass bin = 40 MeV/c^2 and (0.32,1.6) GeV/c^2 are used due to limited statistics

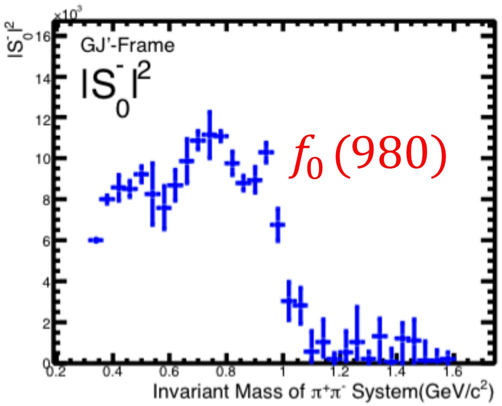

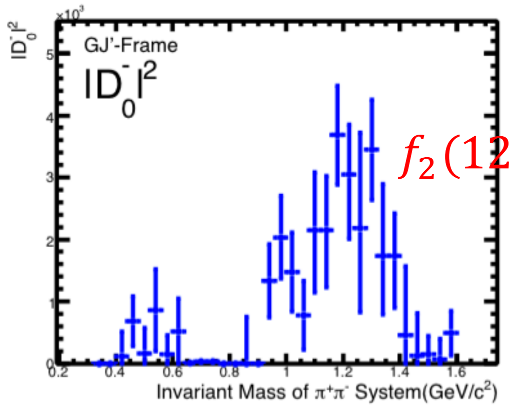

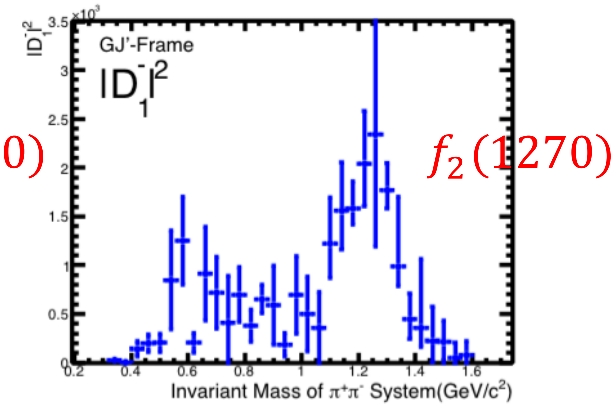

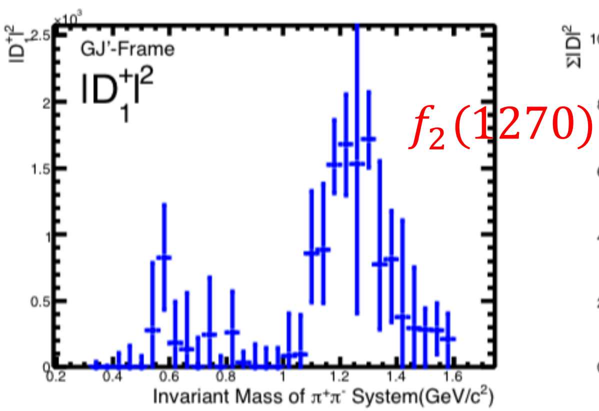

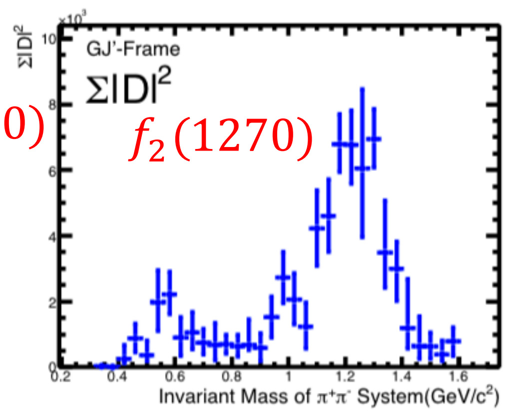

- The $f_0(980)$ and $f_2(1270)$ are appeared in spin 0 and 2 respectively as expected.
- Large continuum background is in S-wave at low mass regions, and there is almost no background in D-waves.
- $f_2(1270)$ is appeared in all D-waves.

Partial wave analysis: mass dependent fit

- Intensities are fitted with coherent background and one Breit-Wigner function

$$F_{\text{fit}} = \left| \underline{\left(a_0 \cdot e^{ia_1}\right)} \cdot \underline{bkg(m)} + a_2 \underline{BW(m)} \right|^2$$

phase factor between background and Breit-Wigner

$$bkg(m) = \sqrt{\frac{q}{m^2}}\, e^{(-b_1 q - b_2 q^2)} \text{ for S-wave}$$

$$bkg(m) = 1 \text{ for D-wave}$$

$$BW(m) = \frac{m\Gamma(m)}{m^2 - m_0^2 - im_0\Gamma(m)},\ \Gamma(m) = \Gamma_0 \frac{q}{m} \frac{B_l^2(q^2R^2)}{B_l^2(q_0^2R^2)}$$

$\boldsymbol{a_0, a_1, a_2, b_1, b_2}$: fit parameters
$\boldsymbol{m_0, \Gamma_0}$: mass and width of resonance (fit parameters)
$\boldsymbol{q}$: breakup momentum
$\boldsymbol{B_l}$: Barrier factor from [1]
$\boldsymbol{R}$: empirical interaction radius (~1fm)

[1] F. Von Hippel and C. Quigg. Centrifugal-barrier effects in resonance partial decay widths, shapes, and production amplitudes. *Phys. Rev.*, D5:624–638, 1972.

Partial wave analysis: mass dependent fit of $|S_0^-|^2$

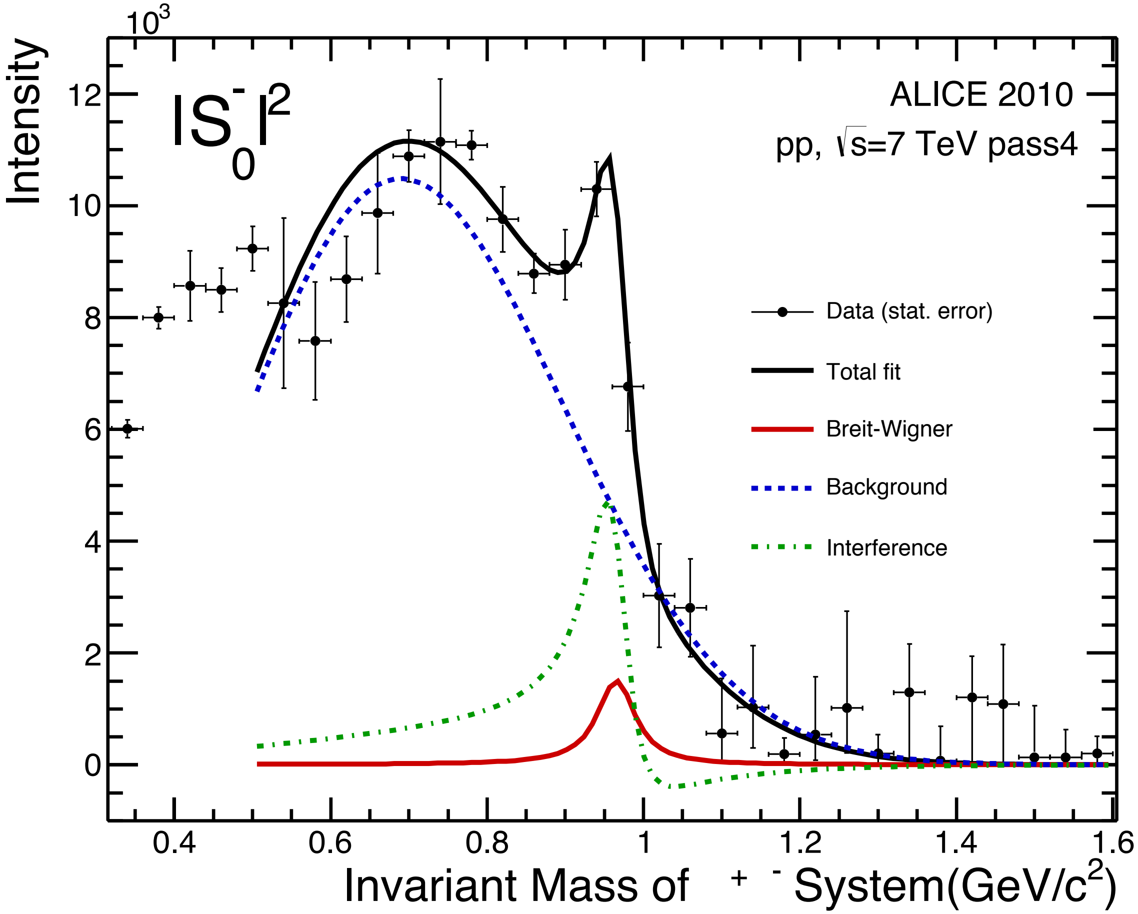

x : Invariant mass of $\pi^+\pi^-$
y : $|S_0^-|^2$

The data is well-fitted with large continuum background and $f_0(980)$ signal. Two functions are interfered each other at $f_0(980)$ regions.

$f_0(980)$	Mass (MeV/c^2)	Width (MeV/c^2)	χ^2/NDF
PDG	980 ± 10	40 to 100	
From fit	$965 \pm 21(stat.)$	$56 \pm 42(stat.)$	1.4

Partial wave analysis: mass dependent fit of $\Sigma|D|^2$

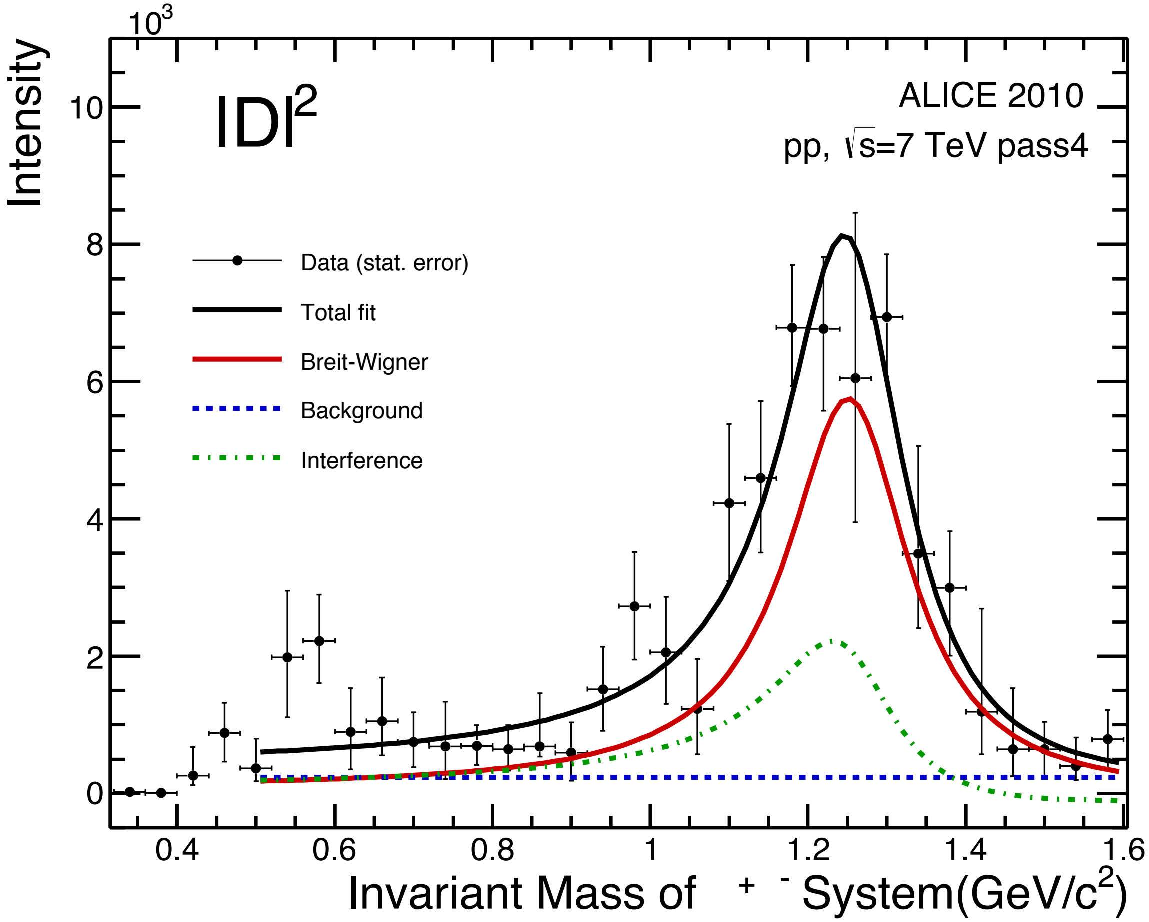

x : Invariant mass of $\pi^+\pi^-$
y :$\Sigma|D|^2$

The data is well-fitted with small constant background and $f_2(1270)$ signal. Two functions are interfered each other.

$f_2(1270)$	Mass (MeV/c^2)	Width (MeV/c^2)	χ^2/NDF
PDG	1275.1 ± 1.2	$185.1^{+2.9}_{-2.4}$	
From fit	$1257 \pm 16(stat.)$	$187 \pm 37(stat.)$	0.94

Conclusions

- Data analysis
  - Double-Pomeron exchange dominates central production at high energies and generates only even multiplicities.
  - ALICE could measure central productions by utilizing double gap topology.
  - $\pi^+\pi^-$ final states are studied with special trackcuts and $f_0(980)$ and $f_2(1270)$ are clearly seen.
  - Currently, purity is estimated as 50% and cross section will be obtained using various MC.
- Partial wave analysis has been done to get properties of produced particles.
  - Spin, mass, and width of produced particles are obtained.

$f_0(980)$	Mass (MeV/c^2)	Width (MeV/c^2)	Spin
PDG	980 ± 10	40 to 100	0
ALICE	$965 \pm 21(stat.)$	$56 \pm 42(stat.)$	0

$f_2(1270)$	Mass (MeV/c^2)	Width (MeV/c^2)	Spin
PDG	1275.1 ± 1.2	$185.1^{+2.9}_{-2.4}$	2
ALICE	$1257 \pm 16(stat.)$	$187 \pm 37(stat.)$	2

  - Systematic uncertainties and cross section of $f_0(980)$ and $f_2(1270)$ will be obtained.

Backup

$\pi^+\pi^-$ invariant mass distribution from other experiments

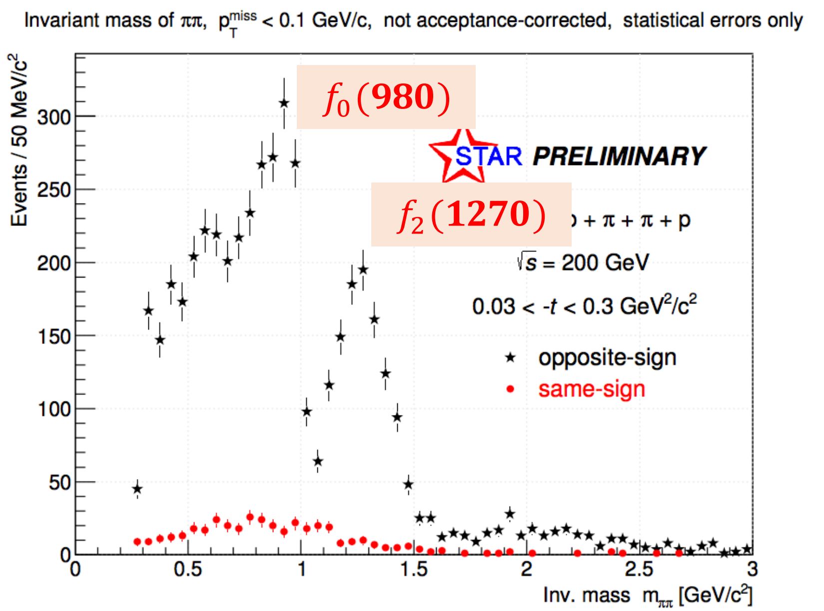

STAR results, Acta Phys.Polon. B47 (2016) 53-58

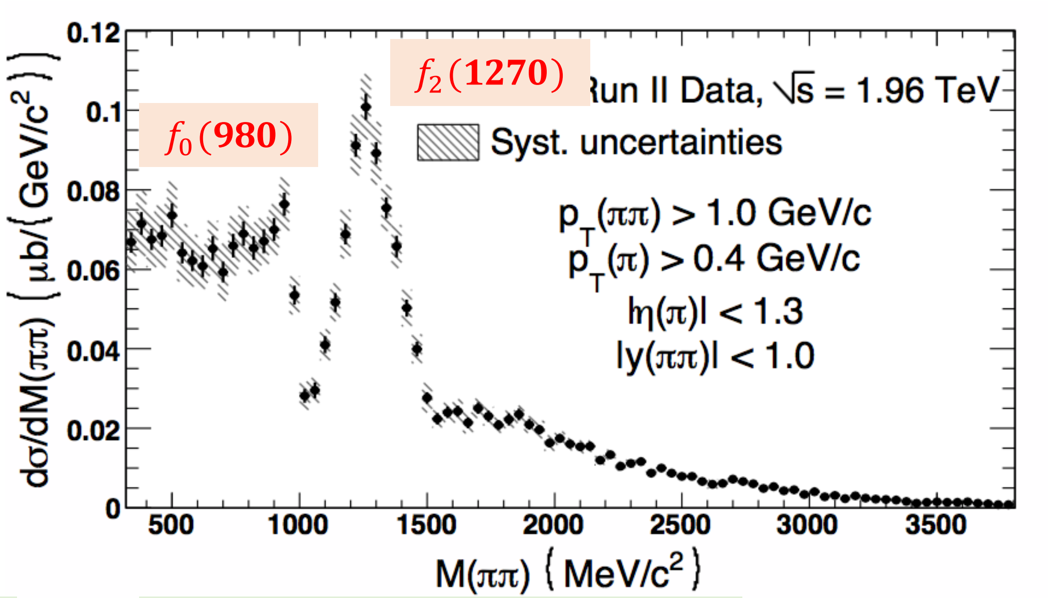

CDF results, arXiv:1502.01391v3

Silicon Pixel Detector (SPD)

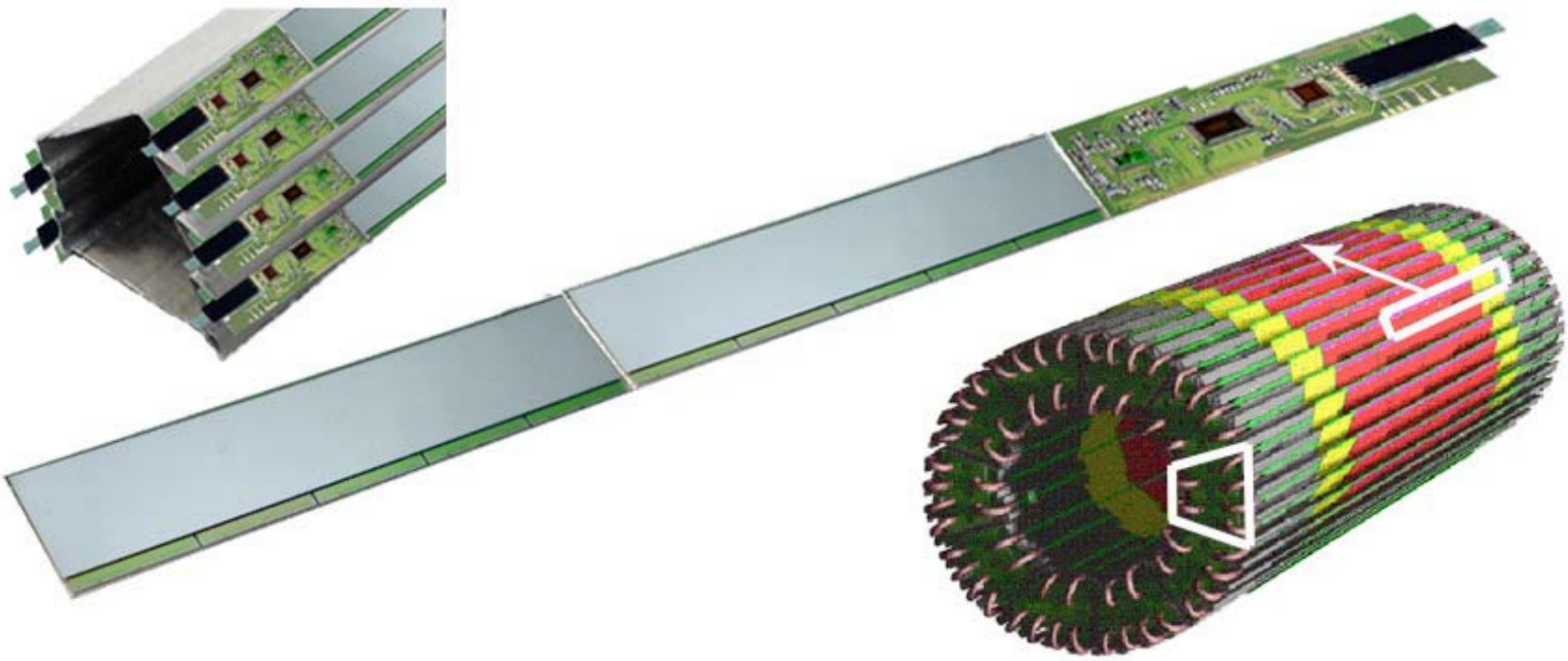

1200 chips
400 at inner and 800 at outer

THE ALICE SILICON PIXEL DETECTOR (SPD), A. KLUGE

Vertex distributions

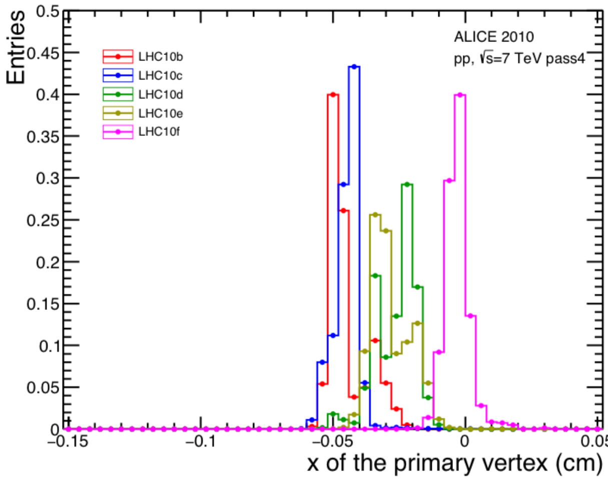

(a) x_{vtx} from the data

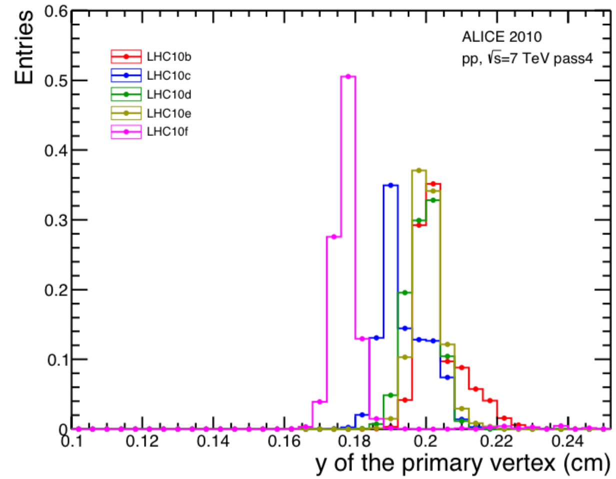

(b) y_{vtx} from the data

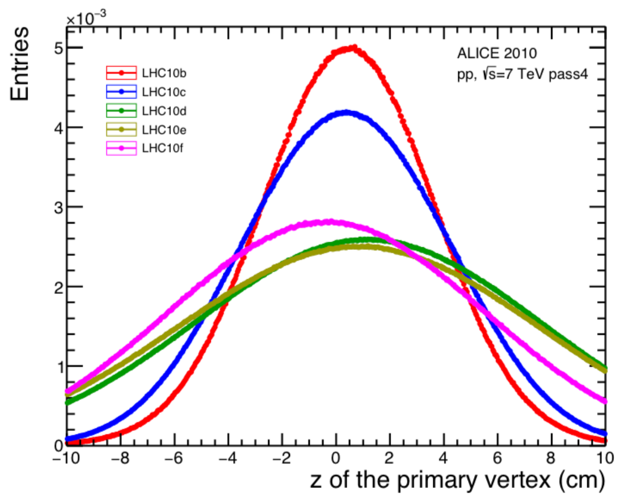

(c) z_{vtx} from the data

SPD clusters versus SPD tracklets cut

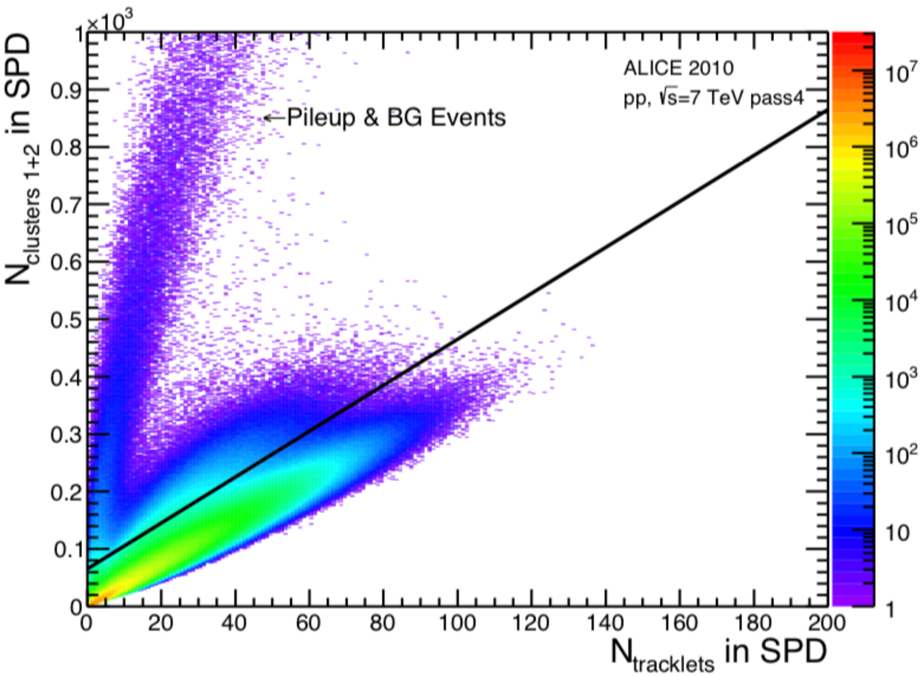

(a) Before cluster cut

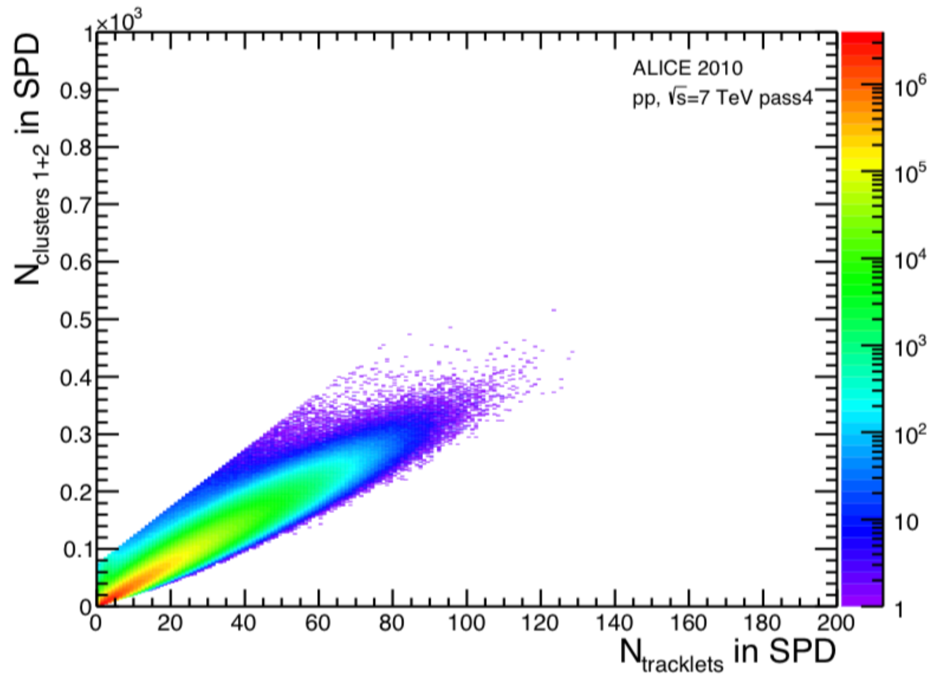

(b) After cluster cut

Rejected events from trackcuts

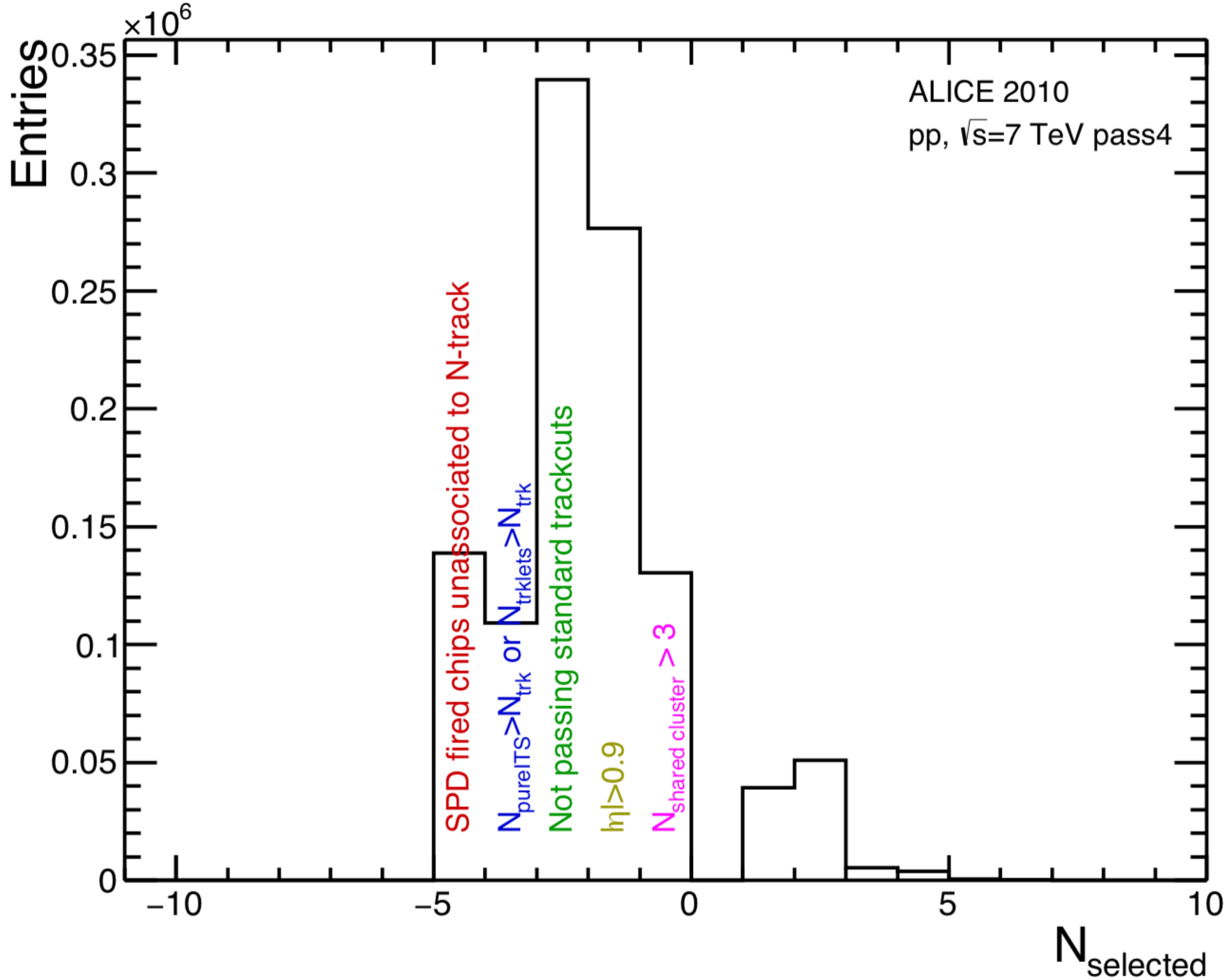

Bayesian probabilities

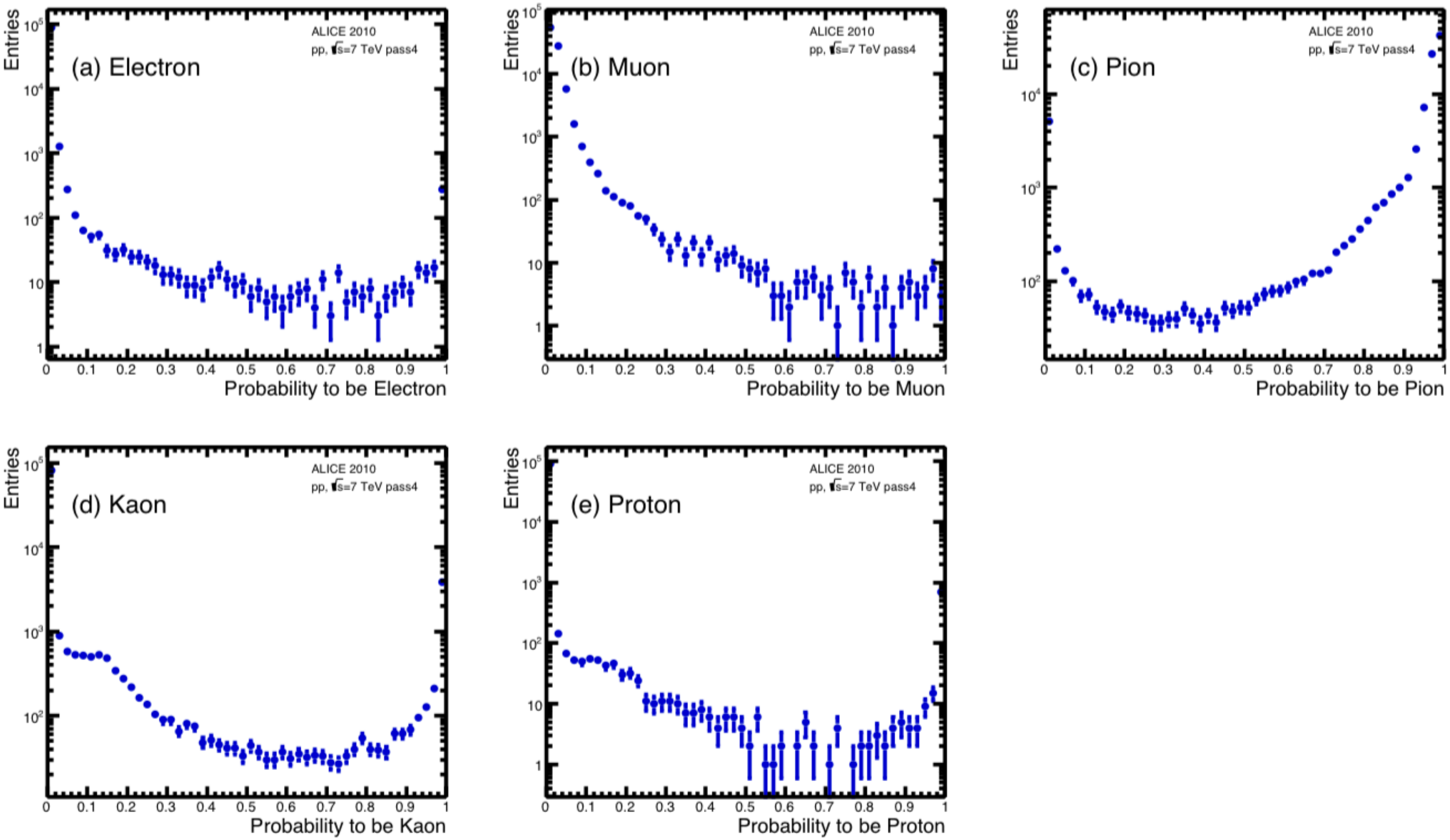

mean p_T versus mass, p_T versus mass

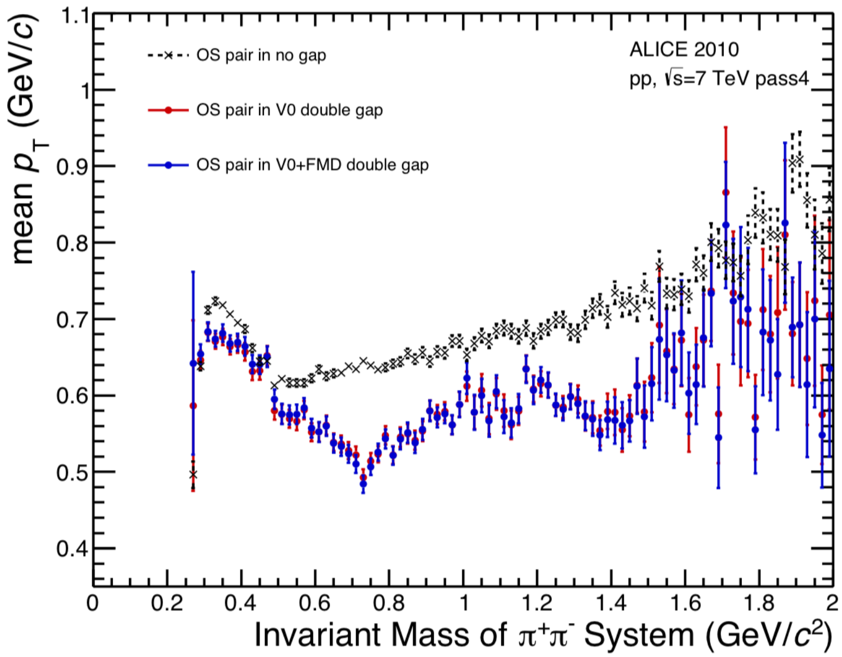

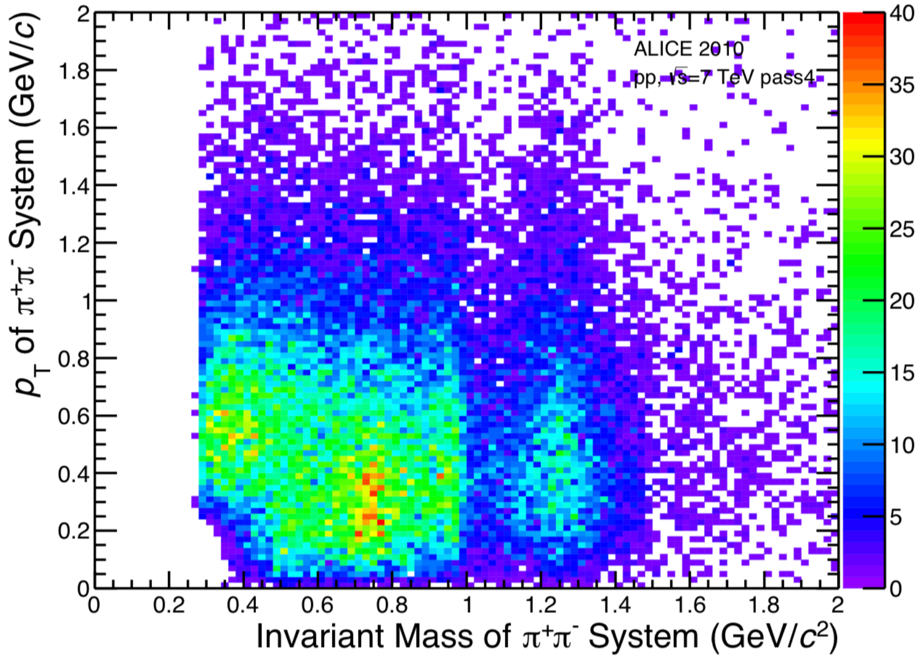

Estimation of background with mother particle

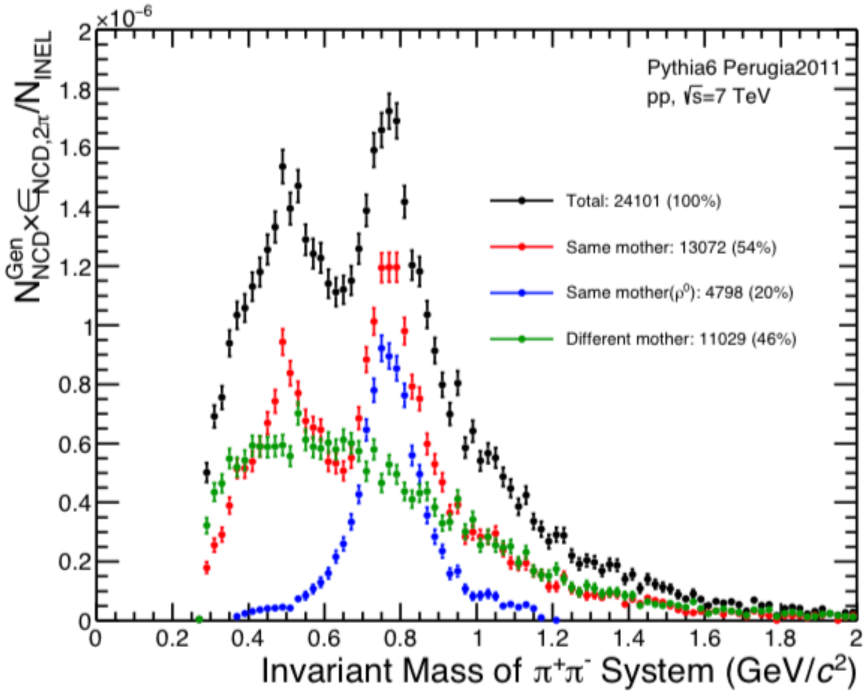

(a) Mass

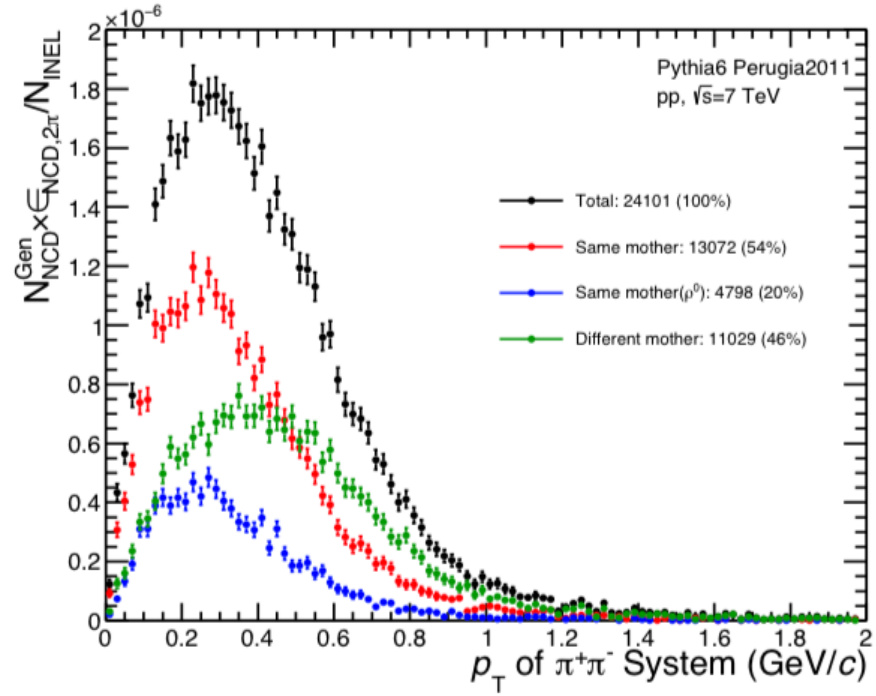

(b) p_T

Differential cross section of DRgen (MC)

$$d\sigma_{p_1 p_2 \to p_1 X p_2} = e^{bt_1}(1-x_1)^{1-2\alpha_{\mathbb{P}}(t_1)} e^{bt_2}(1-x_2)^{1-2\alpha_{\mathbb{P}}(t_2)} \sigma_{\mathbb{P}\mathbb{P}\to X} dx_1 d^2 q_1 dx_2 d^2 q_2$$

b : $8 GeV^{-2}$
t_1, t_2 : Transfer momenta of Pomerons
x_1, x_2 : Feynmann variables of outgoing protons
α_P : Pomeron trajectory, $\alpha_P = 1.08 + 0.25t$
q_1, q_2 : Transverse momenta of outgoing protons

Angular distribution of MC

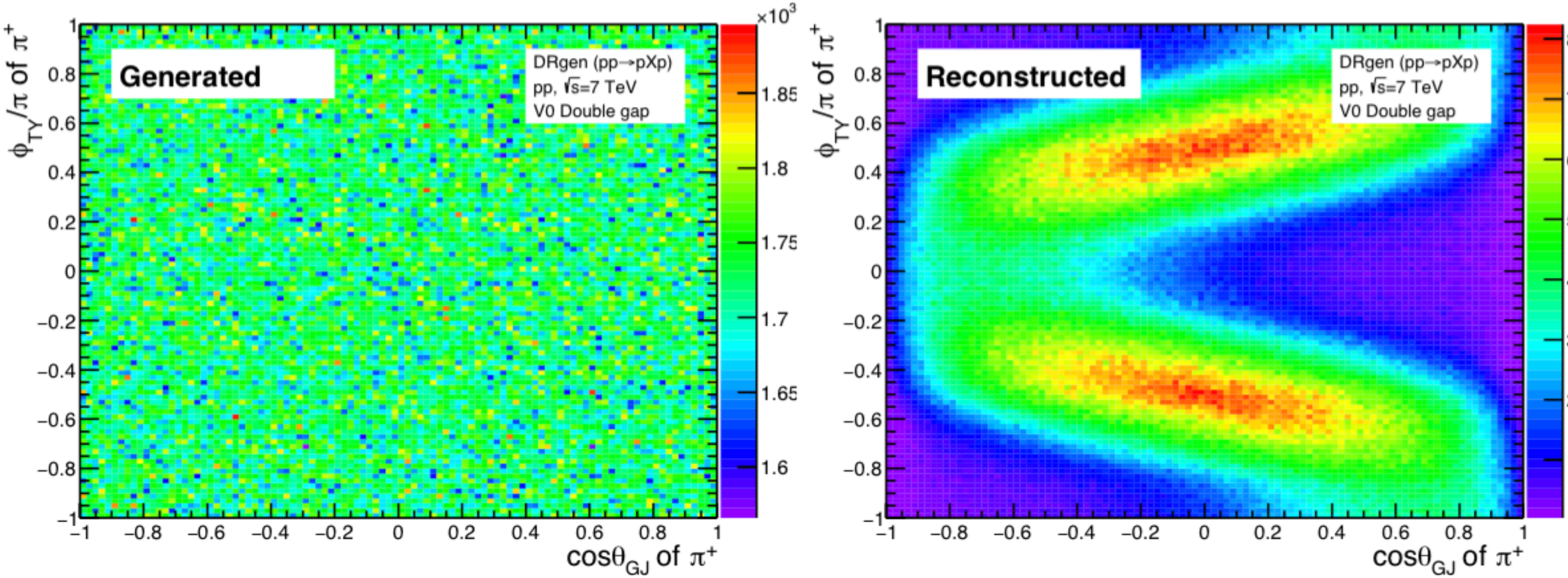

(a) Generated ϕ/π versus $\cos\theta$ of π^+

(b) Reconstructed ϕ/π versus $\cos\theta$ of π^+

PWA based on t_{LM}

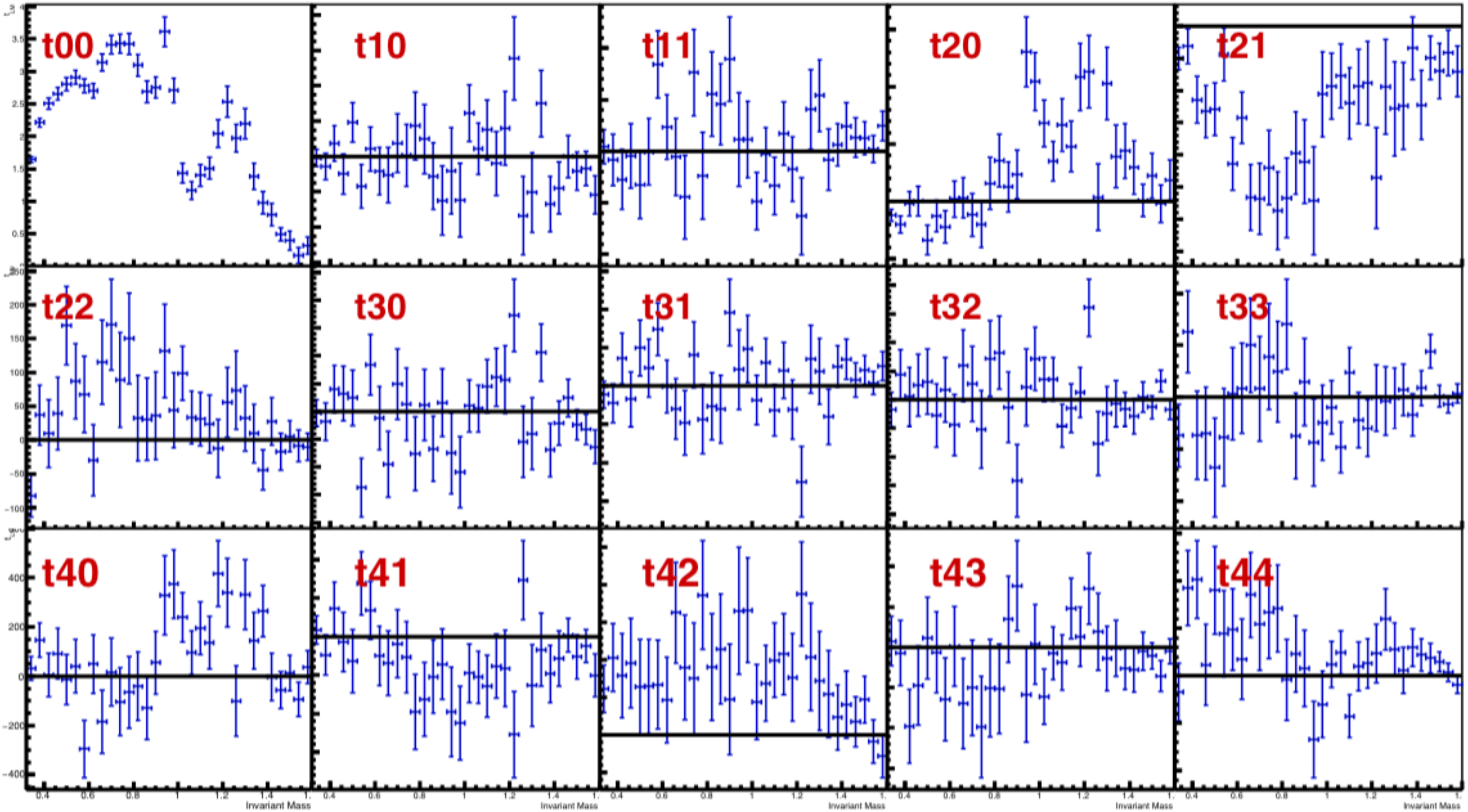

Barrier factor

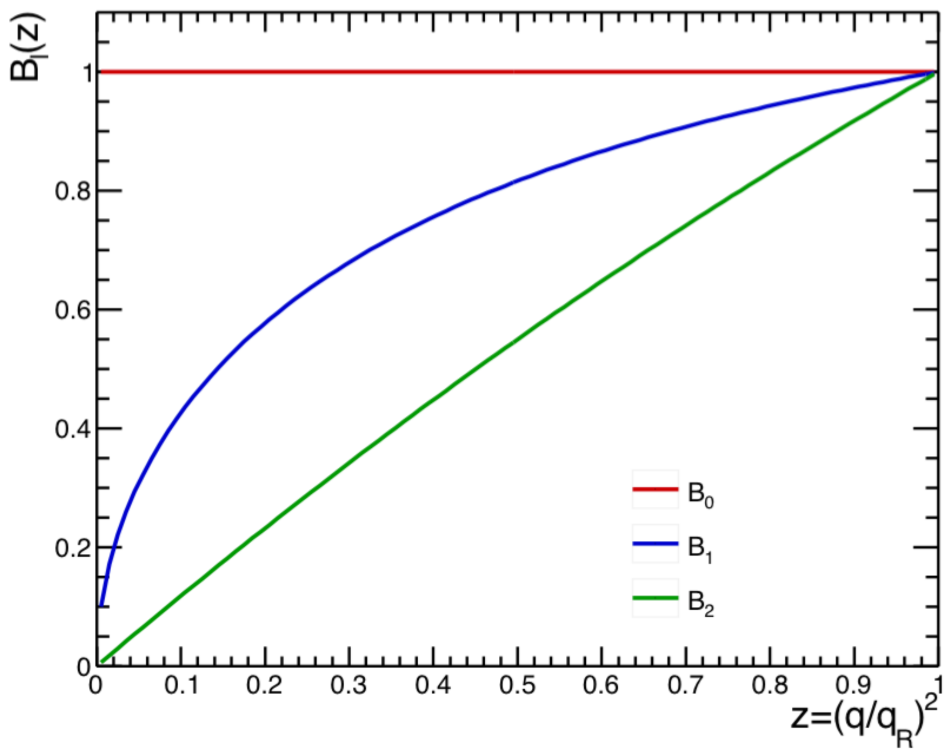

Fig. 3.10: Barrier factor B_l as a function of $z = (q/q_R)^2$ with $l = 0, 1, 2$.

Feynmann diagrams of DPE

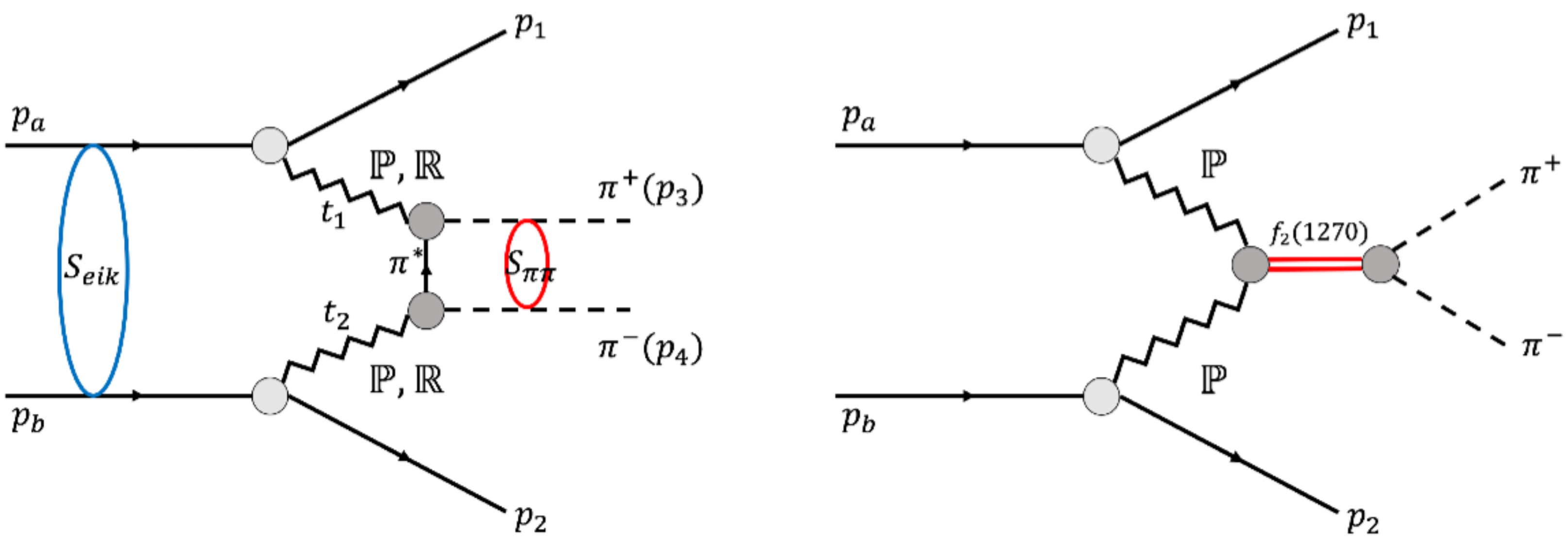

(a) Continuum (b) Resonances

Fig. 1.2: Feynmann diagram of the central diffraction producing dipion system. Both protons are intact only exchanging small momentum transfer $t_1 = (p_a - p_1)^2$, $t_2 = (p_b - p_2)^2$ with Pomeron ($\mathbb{P}$) at high energies. On the left is continuum production of dipion pairs and on the right is resonance production i.e $f_2(1270)$.